AMERICAN UNIVERSITY OF BEIRUT

ANALYSIS ON THE CAPACITY AND OPTIMIZATION FOR D2D UNDERLAYING CELLULAR COMMUNICATIONS USING GEOSTATISTICAL METHODS

by
ALAA TAREK KACHOUH

A thesis
submitted in partial fulfillment of the requirements
for the degree of Master of Engineering
to the Department of Electrical and Computer Engineering
of the Faculty of Engineering and Architecture
at the American University of Beirut

Beirut, Lebanon
April 2016

AMERICAN UNIVERSITY OF BEIRUT

ANALYSIS ON THE CAPACITY AND OPTIMIZATION FOR D2D UNDERLAYING CELLULAR COMMUNICATIONS USING GEOSTATISTICAL METHODS

by

ALAA TAREK KACHOUH

Approved by:

Dr. Youssef Nasser, Associate Professor Electrical and Computer Engineering	Advisor
Dr. Hassan Artail, Professor Electrical and Computer Engineering	Member of Committee
Dr. Zaher Dawy, Professor Electrical and Computer Engineering	Member of Committee

Date of thesis defense: April 22, 2016

AMERICAN UNIVERSITY OF BEIRUT

THESIS, DISSERTATION, PROJECT RELEASE FORM

Student Name: _____Kachouh_____Alaa_____Tarek_____
Last First Middle

⬭ Master's Thesis ⬭ Master's Project ⬭ Doctoral Dissertation

☐ I authorize the American University of Beirut to: (a) reproduce hard or electronic copies of my thesis, dissertation, or project; (b) include such copies in the archives and digital repositories of the University; and (c) make freely available such copies to third parties for research or educational purposes.

☐ I authorize the American University of Beirut, **three years after the date of submitting my thesis, dissertation, or project,** to: (a) reproduce hard or electronic copies of it; (b) include such copies in the archives and digital repositories of the University; and (c) make freely available such copies to third parties for research or educational purposes.

_____

Signature Date

ACKNOWLEDGMENTS

First of all, I would like to express my gratitude to my advisors, Dr. Youssef Nasser and Dr. Hassan Artail. I have been amazingly fortunate to have an advisors who gave me the freedom to explore on my own, and at the same time the guidance to recover when my steps faltered. Their insightful comments and constructive criticism at different stages of my research were though-provoking and they helped me focus my ideas. So I am grateful to them for holding me to a high research standard and enforcing strict validations for each research result. I would also like to thank Dr. Zaher Dawy for being part of the committee and one of the best teachers that I have had.

Second, I would like to thank my family and relatives, particularly my father, and aunts for their continuous support during the good and difficult times during my studies. Without their support it would have been very difficult to arrive at this point.

Finally, I would like to thank my close friends who always stood by me and helped me stay sane through these difficult years. Their support and care helped me overcome setbacks and stay focused on my graduate study. I greatly value their friendship and I deeply appreciate their belief in me.

AN ABSTRACT OF THE THESIS OF

Alaa Tarek Kachouh for Master of Engineering
Major: Electrical and Computer Engineering

Title: Analysis on the Capacity and Optimization for D2D Underlaying Cellular Communications using Geostatistical Methods

Device-to-device (D2D) communication has gained a lot of attention in the last few years, and is considered to be a crucial part of the 4G Long Term Evolution - Advanced (LTE-A) cellular system and Beyond 4G (B4G) systems, introducing flexible, cost and energy efficient solutions. However, one of the limiting factors in such communication scenario is the interference introduced due to the reuse of cellular resources for D2D links, degrading the network's quality of service (QoS) and the transmission capacity. In this thesis, we consider a non-cooperative deployment for the LTE and D2D links and derive closed-form expressions of the ergodic capacities for both systems based on their Signal-to-Interference Ratio (SIR) distributions. We show that the capacities of both D2D and LTE are concave and convex respectively w.r.t the transmitted power ratio. We then propose two optimization algorithms of the power allocation based on the convex concave procedure (CCCP) and a Geo-statistical approach. The CCCP procedure is used to obtain the optimal transmitted power ratio that satisfies the target Quality of Service (QoS) under limited number of D2D links. In crowded D2D environment, we propose to exploit a spatial statistics technique to estimate the Signal-to-Interference plus Noise Ratio (SINR) and interference distributions based on the spatial correlation of the D2D links and cellular links using Kriging interpolator. The resulting information is then incorporated in the power optimization problem to relax the constraints and provide interference-aware solution for such scenario. The analytical and numerical results demonstrate the effectiveness of the introduced algorithms and show that there exists an optimal power ratio that satisfies the transmission constraints in both D2D and cellular systems.

CONTENTS

ILLUSTRATIONS

Figure Page

TABLES

ABBREVIATIONS

WWRF	Wireless World Research Forum
3GPP	Third-Generation Partnership Project
D2D	Device-to-Device
ProSe	Proximity-Based Services
BS	Base Station
QoS	Quality of Service
UEs	User Equipment
i.i.d	Independent and identically distributed
ISM	Industrial, Scientific and Medical
DRX	Device-to-Device Receiver
DTX	Device-to-Device Transmitter
LTE	Long Term Evolution
SIR	Signal to Interference Ratio
CCCP	Convex Concave Procedure
SINR	Signal to Interference plus Noise Ratio
TID	Tolerant Interference Degree
DL	Downlink
UL	Uplink
ILA	Interference Limited Area
CSI	Channel State Information
CUE	Cellular User Equipment
PDF	Probability Density Functions
RV	Rrandom Variables
CDF	Cumulative Distribution Function
CCDF	Complementary Cumulative Distribution Function
IDW	Inverse Distance Weighting
PPP	Poisson Point Process
OKE	Ordinary Kriging Estimator

CHAPTER I

INTRODUCTION

A. Motivation

The introduction of smart phones and their applications have caused a tremendous burden on the cellular networks with the ever exploding voice and data traffic consumption. The Wireless World Research Forum (WWRF) had estimated about 7 trillion wireless devices serving 7 billion people by 2020 [1], leading then to the so-called spectrum crisis. Given the drastic growth of bandwidth hungry applications, such as video streaming and multimedia file sharing, coupled with the limitations of the current cellular systems which already have been pushed [1], the time has come to find innovative methods to accommodate these bandwidth consuming applications and services within the network's capacity. Although the deployment of small cells, such as femto-cells, can bring better coverage and higher rates, it could cause heavy interference in loaded networks.

The Third-Generation Partnership Project (3GPP) has defined data offloading as an alternative solution to cope with this problem, where the 3GPP SA1 (services) working group has been studying since 2011 a new Rel-12 item, named Study on Proximity-Based Services (ProSe), targeting the potential requirements for an operator to integrate Device-to-Device (D2D) communication in their network [3]. This technology has been proposed as a promising concept for improving user experiences and resource utilization in cellular networks by taking advantage of users' proximity.

B. D2D Background

Recently, D2D communications underlying cellular networks have received great attention in the research community, and it was first introduced in [2] to provide a multihop relay architecture for cellular networks, which was then studied as a potential spectral efficiency enhancement. Later on, it was investigated as a promising spectrum sharing component that could offer further benefits such as reliability, flexibility, power saving and plug-and-play capabilities[3],[4].

The term D2D communications refers to direct short-range communications between terminals of a mobile network, without the intermediate transmission to a Base Station (BS). What differentiates it from conventional approaches, such as Bluetooth and Wi-Fi Direct, is the utilization of licensed spectrum with QoS guarantees, while no manual network detection-selection is required [5].

Basically, the direct communication between nearby mobile devices will offload the base station and help reduce the overhead and this will improve spectrum utilization, overall throughput, and energy efficiency, while enabling new peer-to-peer and location-based applications and services. Potential application scenarios include, among others, proximity-based services where devices detect their proximity and subsequently trigger different services (such as social applications triggered by user proximity, advertisements, local exchange of information, smart communication between vehicles, etc.). Other applications include public safety support, where devices provide at least local connectivity even in case of damage to the radio infrastructure. Examples on the applications for D2D can be shown in Figure 1.1.

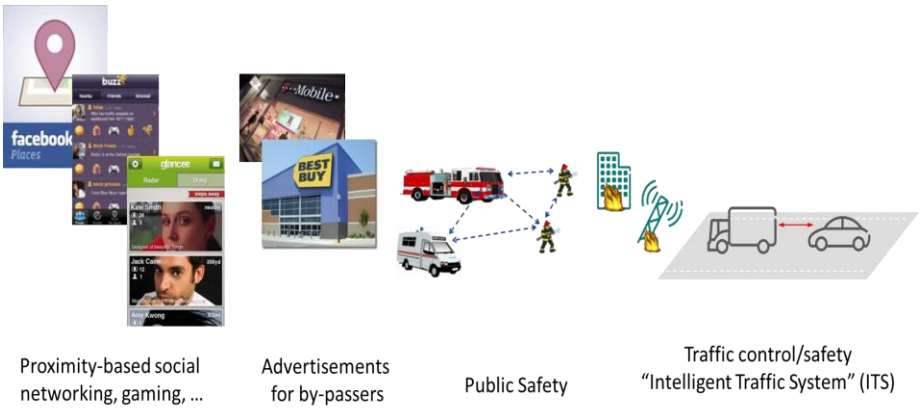

Figure 1.1 Example application scenarios for Device to Device [3]

C. D2D communication classification

D2D communications are divided into two types; the in-band type and the out-band type. The former operates in licensed bands, while the latter operates in license-free bands [6].

In in-band D2D communications, User Equipments (UEs) communicate over a direct link using the same spectrum as the cellular resources. This allows the users to communicate directly without the need to go through the BS, except in some cases for signalling purposes. Hence, the overall throughput of served users will increase. This however is obtained at the detriment of increased interference due to the reutilization of the cellular resources for D2D links [7].

In-band communications are divided into underlay and overlay categories. As the name implies, underlay communications suggests D2D and cellular communications share the same available resources. On the other hand, in overlay mode, the D2D communication is carried out using dedicated resources from the cellular resources. The major drawback of this mode is the heavy interference sensed by both networks.

To eliminate such interference, one way is to operate in out-band D2D mode, where D2D links use the 2.4 GHz ISM band for their communications. Such communication usually requires special non-LTE interfaces such as Wi-Fi Direct and Bluetooth/ZigBee. Although the interference among D2D and cellular is irrelevant in this mode, the D2D links are exposed to uncontrolled nature of the unlicensed spectrum [5]. Out-band is also divided further into controlled and autonomous categories which are self-explanatory from their names. Since the interference in out-band is hard to manage, in our work we will focus on the in-band underlay mode.

The D2D operation modes and their categories are illustrated in Figure 1.2

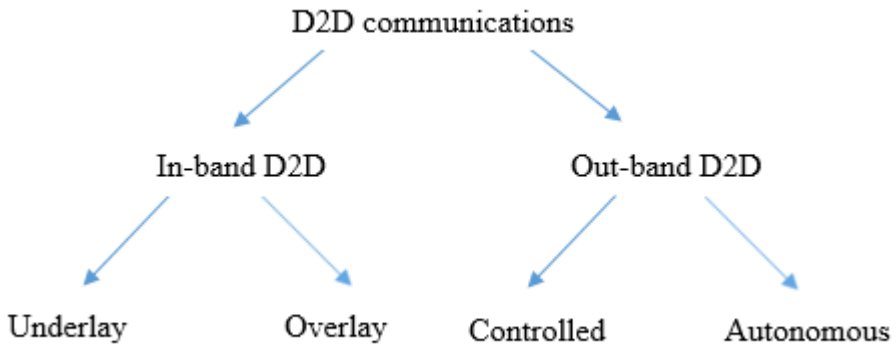

Figure 1.2 D2D communication classification

Interference between the cellular and D2D communications is the most important issue in underlaying D2D communications. Good interference management algorithms can increase the system capacity, and have attracted a lot of attention [8]. Generally interference management schemes are classified into three categories [9]:

1. Interference avoidance: communication is done in an orthogonal fashion, hence avoiding unwanted interference between D2D and cellular links.

2. Interference coordination: interference is controlled by implementing smart power control or/and resource allocation.
3. Interference cancellation: advanced coding and decoding techniques are done at the cellular and D2D links to remove the interference from the intended signals.

In this work, we will be assuming D2D operation on the downlink band and thus, the main interference is originated from the Base Station (BS) to Device-to-Device Receiver (DRXs), interference from Device-to-Device Transmitters (DTXs) to Cellular UEs and adjacent D2D links interference. Such communication scenario can be visualized in Figure 1.3.

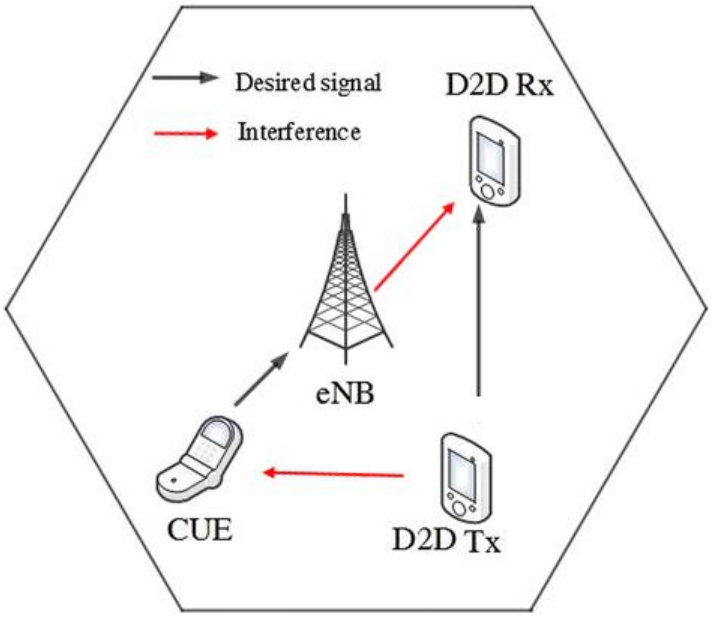

Figure 1.3 D2D and cellular networks sharing resources

D. Objective and Related Work

This thesis targets the coexistence of D2D and Long Term Evolution (LTE) cellular networks, where we consider a non-cooperative deployment for the LTE and D2D links and derive closed-form expressions of the ergodic capacities for both

systems based on their Signal to Interference Ratio (SIR) distributions. We show that the capacities of both D2D and LTE are concave and convex respectively w.r.t the transmitted power ratio. We then propose two optimization algorithms of the power allocation based on the Convex Concave Procedure (CCCP) and a Geo-statistical approach. The CCCP procedure is used to obtain the optimal transmitted power ratio that satisfies the target QoS under limited number of D2D links. In crowded D2D environment, we propose to exploit a spatial statistics technique known as Ordinary Kriging Estimator (OKE) to estimate the Signal to Interference plus Noise Ratio (SINR) and interference distributions based on the spatial correlation of the D2D links and cellular links. The resulting information is then incorporated in the D2D power optimization problem to relax the constraints and provide interference-aware solution. The analytical and numerical results demonstrate the effectiveness of the introduced algorithms and show that in the scenario of D2D underlaying cellular communication there exists an optimal power ratio that satisfies the transmission constraints in both D2D and cellular systems.

The transmission capacity is a metric that has been extensively investigated in the literature, as it is considered to be a fundamental issue in heterogeneous systems. Comprehensive analysis has been done in [10] for the transmission capacity of relay assisted D2D networks, where the authors provide a theoretical analysis on the optimal transmission rate over Rayleigh fading channels, firstly by using stochastic geometry, then formulating an optimization problem maintaining the outage probability of both cellular and D2D networks.

The authors in [12] proposed a network controlled algorithm with low computation complexity to efficiently solve the capacity optimization problem in D2D underlay operation where the BS has total channel awareness. In their work, the authors proposed a feasibility function indicating the reusability of D2D for a certain resource in binary operation, in other words, the algorithm tries to give high priority for users who have the least feasible option. The main drawback of this algorithm is the need to have full channel gain knowledge in order to search for the optimal global solution.

An interference mitigation scheme in presented in [13] where the authors aimed at improving the overall capacity and spectral efficiency for a D2D communication in cellular networks. They defined a metric, Tolerant Interference Degree (TID) to evaluate the permissible interference scope for successful D2D transmission; in addition, they derive a lower bound on neighbor distance for a D2D UE.

An interference management strategy which is named as $\delta_D -$ Interference Limited Area (ILA) control scheme was proposed in [14] to enhance the overall capacity of cellular networks and D2D underlaying system. Moreover, an expression of lower bound of ergodic capacity which considers interference from more than one Cellular UE (CUE) is used to analyze the capacity performance of the proposed interference management strategy. However, in [14], only the capacity performance of reusing UL radio resource and the interference control scheme in Uplink (UL) mode are discussed, the case of Downlink (DL) mode is unavailable.

In the rest of this report, Chapter II derives a closed-form expressions on the global ergodic capacity for D2D underlay operation in the DL and provide analytical observations and simulations. Chapter III formulates the problem of capacity optimization and proposes the CCCP approach for tackling it based on the derived expressions. Chapter IV discusses the use of kriging in the optimization of the global capacity of D2D and cellular networks by proposing an algorithm that returns the optimal transmit powers for the D2D TXs while preserving the predefined QoS constraints. And finally, Chapter V concludes the report and presents directions for future work.

CHAPTER II

DERIVATION AND ANALYSIS OF THE GLOBAL ERGODIC CAPACITY IN D2D UNDERLAYING CELLULAR SYSTEM

The target of this chapter is to provide closed-form expressions of the capacities for both D2D and LTE systems. In this work, we assume no channel state information (CSI) is available at the transmitter side. In addition, we assume an interference-limited scenario, i.e. the effect of the thermal noise is very small compared to the interference power level from the neighbouring devices.

A. System model

We consider a basic scenario where several D2D communication sessions coexist with an LTE cellular network. The cellular network consists of a BS and a single LTE CUE, while the D2D network consists of *N* D2D links working on the DL resources. Figure 2.1 shows such a deployment for the devices in a macrocell environment. DTX_k is the k^{th} D2D transmitter, while DRX_k is the k^{th} D2D receiver. The channel gains from BS to CUE and from DTX_k to DRX_k $(k = 1,2,..,N)$ are assumed to be independent and identically distributed (i.i.d) with Rayleigh fading distribution. For the sake of clarification, we assume the following:

1. The transmit power of DTXs are identical and is upper bounded.
2. The channel coefficients are slowly varying for the time period of interest.

3. A simple path loss model is considered, i.e. the TX-RX power relation is given by: $PL = d^{-\alpha}$, where α is the path-loss exponent and d is the distance separation.

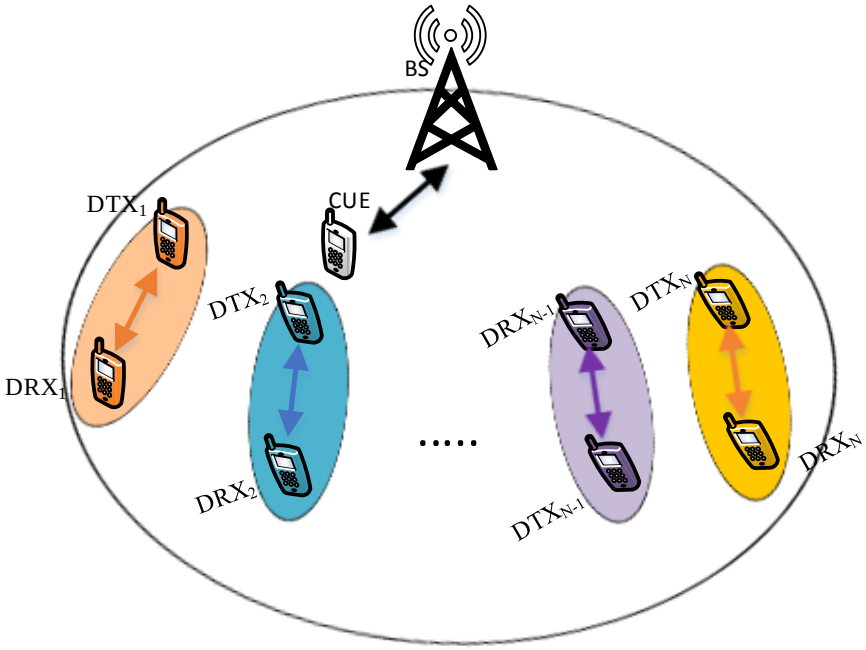

Figure 2.1 Network model of Macro BS with one CUE and several D2D links

B. SIR Distribution

The SINR of the CUE and the k^{th} DRX on the n^{th} resource block can be respectively expressed as:

$$\gamma_c = \frac{P_b\, l_c |h_c|^2}{\sum_{i=1}^{N} P_d\, l_i |h_i|^2 + N_0} \tag{1}$$

$$\gamma_k = \frac{P_d\, l_k |h_k|^2}{\sum_{\substack{j=1 \\ j \neq k}}^{N} P_d\, l_j \left|h_j\right|^2 + P_b\, l_b |h_b|^2 + N_0} \tag{2}$$

where

- P_b is the transmit powers of the BS.
- P_d is the transmit powers k^{th} D2D TX.
- h_k is the channel fading coefficient for the target D2D RX.
- h_j is the channel fading coefficient for interfering D2D TXs on D2D RX.
- h_i is the channel fading coefficient for interfering D2D TXs on CUE.
- h_b is the channel fading coefficient for interfering BS on D2D RX.
- h_c is the channel fading coefficient for the target CUE.
- l_k, l_j, l_i, l_b and l_c are the corresponding path loss attenuations.
- N_0 is the noise variance.

The distributions of the SIR are needed later to obtain the ergodic capacity. Since $|h_c|^2, |h_i|^2, |h_k|^2, \ |h_j|^2$ and $|h_b|^2$ are exponentially distributed, the Probability Distribution Functions (PDFs) of the SIRs is proved below.

The global ergodic capacity, in Bits/Sec/Hz is calculated by averaging over the fading distributions as follows:

$$C_{global} = E_h[log_2(1+\gamma_c)] + E_h[log_2(1+\gamma_k)] \quad (3)$$

where γ_c and γ_k are the SINR given by (1) and (2). *E(.)* is the expected value over the fading distributions respectively. For simplicity, and since the scenario is interference limited, we neglect the thermal noise compared to the interference part in the SINR. We should mention that even though the simplification of the SINR to SIR might seem impractical but this gives us some insights about the capacity expression and evolution.

Furthermore, the robustness of this approximation will be verified in the results section. To the best of our knowledge, there is no previous work dealing with the capacity and SIR distributions. Hence, the problem of the ergodic capacity evaluation turns out to find the SIR distribution followed by an expectation over the channel gain *h*.

In other words, to derive the global capacity in (3), an integration over all *h* is required. Instead, one could replace this integration by a simpler expression by integrating over SINR or SIR. The capacity will be then equivalent to:

$$C_{global} = E_{\tilde{\gamma}_c}[log_2(1+\tilde{\gamma}_c)] + E_{\tilde{\gamma}_k}[log_2(1+\tilde{\gamma}_k)] \tag{4}$$

where $\tilde{\gamma}_c$ and $\tilde{\gamma}_k$ are the SIR of D2D and CUE respectively. Using (4), the global ergodic capacity of both D2D and CUE could be obtained if the PDF of the SIR are given. Hence, the problem turns out to find these pdf as done in [14]**.**

Lemma 1 *At a given location and in Rayleigh fading channel, the distributions of SIRs s at a CUE and k[th] D2D links are given by:*

$$p_{\tilde{\gamma}_c}(s) = P_b l_c \left[\prod_{i=1}^{N} \frac{1}{P_d l_i}\right] \sum_{j=1}^{N} \frac{\left(P_d l_j\right)^2}{\prod_{\substack{k=1 \\ k\neq j}}^{N} \left(\frac{1}{P_d l_k} - \frac{1}{P_d l_j}\right) \left(P_d l_j s + P_b l_c\right)^2} \tag{5}$$

$$p_{\tilde{\gamma}_k}(s) = \frac{1}{P_d l_k P_b l_b} \left[\prod_{i=1}^{N} \frac{1}{P_d l_i}\right] \times \left[\sum_{j=1}^{N} \frac{\left(P_d l_k P_d l_j\right)^2}{\left(\prod_{\substack{u=1 \\ u\neq j}}^{N} \left(\frac{1}{P_d l_u} - \frac{1}{P_d l_j}\right)\right) \left(\frac{1}{P_b l_b} - \frac{1}{P_d l_j}\right) \left(P_d l_j s + P_d l_k\right)^2} + \frac{\left(P_d l_k P_b l_b\right)^2}{\left(\prod_{\substack{u=1 \\ u\neq j}}^{N} \left(\frac{1}{P_d l_u} - \frac{1}{P_b l_b}\right)\right) \left(P_b l_b s + P_d l_k\right)^2}\right] \tag{6}$$

Proof: We focus on the distribution of the SIR at the CUE receiver. Let us define the two following Random Variables (R.Vs): $X = P_b\, l_c|h_c|^2$ and $Y = \sum_{i=1}^{N} P_d\, l_i|h_i|^2$ with PDF given by:

- $X \sim \frac{1}{P_b\, l_c} e^{-\frac{x}{P_b\, l_c}}$
- $Y \sim \left[\prod_{i=1}^{N} \frac{1}{P_d l_i}\right] \left[\sum_{j=1}^{N} \frac{e^{-\frac{x}{P_d l_k}}}{\prod_{\substack{k=1 \\ k\neq j}}^{N} \left(\frac{1}{P_d l_k} - \frac{1}{P_d l_j}\right)}\right]$

By applying the change of variable theorem as follows:

$$\begin{cases} S = X/Y \\ T = Y \end{cases} \Leftrightarrow \begin{cases} X = ST \\ T = Y \end{cases} \tag{7}$$

The joint PDF for the couple (S, T) can be written as:

$$f_{ST}(s,t) = f_{XY}(x(s,t), y(s,t))|J(s,t)| \tag{8}$$

where $J(s,t)$ is the Jacobian of the transformation depending on the new variables. As X and Y are independent, we obtain:

$$f_{ST}(s,t) = f_{XY}(st,t)|t| = \frac{|t|}{P_b\, l_c}\left[\prod_{i=1}^{N} \frac{1}{P_d l_i}\right] \sum_{j=1}^{N} \frac{e^{-t\left(\frac{s}{P_b\, l_c} + \frac{1}{P_d l_j}\right)}}{\prod_{\substack{k=1 \\ k\neq j}}^{N} \left(\frac{1}{P_d l_k} - \frac{1}{P_d l_j}\right)} \tag{9}$$

By integrating the above joint PDF w.r.t the variable t, we obtain the SIR at the LTE cellular receiver:

$$\begin{aligned} f_{\tilde{\gamma}_c}(s) &= \int_0^{\infty} f_{ST}(s,t)\, dt \\ &= P_b l_c \left[\prod_{i=1}^{N} \frac{1}{P_d l_i}\right] \sum_{j=1}^{N} \frac{\left(P_d l_j\right)^2}{\prod_{\substack{k=1 \\ k\neq j}}^{N} \left(\frac{1}{P_d l_k} - \frac{1}{P_d l_j}\right) \left(P_d l_j s + P_b l_c\right)^2} \end{aligned} \tag{10}$$

$f_{\widetilde{\gamma}_k}$ is obtained by following the same steps as previously shown, and the proof is complete.

C. Ergodic Capacity

We can show that the global ergodic capacity of the regular cellular communication and D2D communications is respectively equal to:

$$C_{global} = C_{cell} + C_{D2D} \tag{11}$$

where

$$C_{cell} = P_b l_c \left[\prod_{i=1}^{N} \frac{1}{l_i}\right] \times \sum_{j=1}^{N} \frac{l_j}{\prod_{\substack{k=1 \\ k\neq j}}^{N} \left(\frac{1}{l_k} - \frac{1}{l_j}\right)\left(P_d l_j - P_b l_c\right)} log_2\left(\frac{P_d l_j}{P_b l_c}\right) \tag{12}$$

and

$$C_{D2D} = \frac{P_d^{2-N} l_k}{P_b l_b}\left[\prod_{i=1}^{N} \frac{1}{l_i}\right] \times \left[\sum_{j=1}^{N} \frac{P_d^{N-2} l_j}{\left(\prod_{\substack{u=1 \\ u\neq j}}^{N} \left(\frac{1}{l_u} - \frac{1}{l_j}\right)\right)\left(\frac{1}{P_b l_b} - \frac{1}{P_d l_j}\right)\left(l_j - l_k\right)} log_2\left(\frac{l_j}{l_k}\right) + \frac{P_b l_b}{\prod_{i=1}^{N}\left(\frac{1}{P_d l_i} - \frac{1}{P_b l_b}\right)\left(P_b l_b - P_d l_k\right)} log_2\left(\frac{P_b l_b}{P_d l_k}\right)\right] \tag{13}$$

Proof: By substituting the distributions of the SIRs derived in Lemma 1 in (4) and [15], we obtain the ergodic capacities.

1. ***Special case: Major interfering links***

As the expressions of (12) and (13) are too complex to interpret, we focus in this section on the case where the two major interfering D2D links with the cellular system are only considered. Indeed, in such a heterogeneous scenario (i.e. cellular and D2D links), only few D2D links will affect the overall system capacity as the latter depends on the distance between the D2D links from one side and on the distance between the cellular and D2D receivers from the other side. Hence, we assume that only the closest two D2D links will affect a particular cellular receiver, as seen in Figure 2.2.

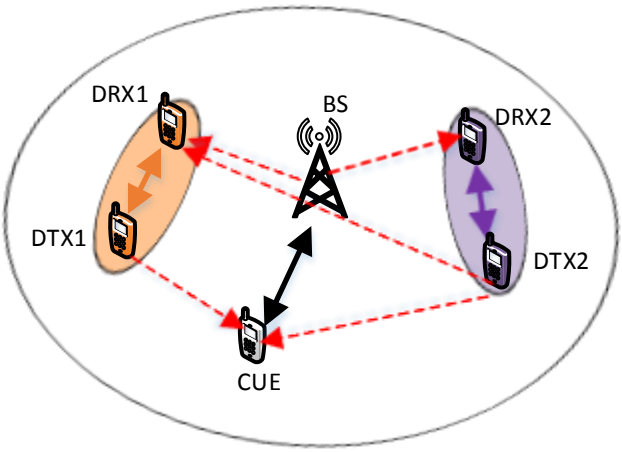

Figure 2.2 Special case deployment scenario

Hence, when $N = 2$, the SIR expression of the D2D link becomes:

$$\tilde{\gamma}_k = \frac{P_d \, l_k |h_k|^2}{P_d l_d |h_d|^2 + P_b \, l_b |h_b|^2} \tag{14}$$

and the SIR for the CUE is given by:

$$\tilde{\gamma}_c = \frac{P_b \, l_c |h_c|^2}{P_d (l_{d1} |h_{d1}|^2 + l_{d2} |h_{d2}|^2)} \tag{15}$$

where

- h_d is the channel fading coefficients for the interfering link on the D2D target link.
- h_{d1} is the channel fading coefficients for the interfering D2D links 1 on the target CUE.
- h_{d2} is the channel fading coefficients for the interfering D2D links 2 on the target CUE.
- l_d, l_{d1}, l_{d2} are their corresponding path-loss attenuations.

The global ergodic capacity will be then written as ((11),(12)):

$$C_g(P,l) = \quad C_{cell}(P,l) + \ C_{D2D}(P,l) \tag{16}$$

where

$$C_{cell}(P,l) = P_b l_c \left[\prod_{i=1}^{2} \frac{1}{l_i}\right] \times \sum_{j=1}^{2} \frac{l_j}{\prod_{\substack{k=1 \\ k\neq j}}^{2} \left(\frac{1}{l_k} - \frac{1}{l_j}\right)\left(P_d l_j - P_b l_c\right)} log_2\left(\frac{P_d l_j}{P_b l_c}\right) \tag{17}$$

and

$$C_{D2D}(P,l) = \frac{l_k}{l_d} \times \left[\frac{log_2\left(\frac{l_d}{l_k}\right)}{\left(1 - \frac{P_b l_b}{P_d l_d}\right)\left(1 - \frac{l_k}{l_d}\right)} + \frac{\log_2\left(\frac{P_b l_b}{P_d l_k}\right)}{\left(\frac{P_b l_b}{P_d l_d} - 1\right)\left(1 - \frac{P_d l_k}{P_b l_b}\right)}\right] \tag{18}$$

where (17) is the capacity of the cellular system, i.e. C_{cell}, and (18) represents the capacity of the D2D system. As seen in (17) and (18), we notice both expressions depend on the path loss and power components. Hence, to further simplify the global expression, we reformulate it as follows:

$$C_g(\beta_1, \beta_2) = \left[\frac{log_2\beta_1}{(\beta_1 - 1)\left(1 - \frac{A_3}{A_1}\right)} + \frac{log_2\beta_2}{(\beta_2 - 1)\left(1 - \frac{A_1}{A_3}\right)}\right] + \left[\frac{log_2\frac{A_1}{A_2}}{\left(1 - \frac{A_2}{\beta_1}\right)\left(\frac{A_2}{A_1} - 1\right)} + \frac{log_2\frac{A_3}{\beta_2}}{\left(\frac{A_3}{\beta_2} - \frac{A_1}{A_2}\right)\left(1 - \frac{\beta_2}{A_3}\right)}\right] \quad (19)$$

where

- $\beta_1 = P_d l_{d1}/P_b l_c$
- $\beta_2 = P_d l_{d2}/P_b l_c$
- $A_1 = l_{d1} l_b/\mathrm{l}_c l_k$
- $A_2 = l_{d1} l_b/l_c l_d$
- $A_3 = l_{d2} l_b/l_c l_k$

The parameters β_1 and β_2 capture the transmit power ratio of both cellular and D2D systems, i.e. P_d and P_b. It is noted that (19) is defined for all excluding the following:

1. $\beta_1, \beta_2 \neq 1$
2. $A_2, A_3 \neq A_1$
3. $A_3 \neq \beta_2$
4. $A_2 \neq \beta_1$

D. Performance Evaluation and Analysis

In this section, the obtained global ergodic capacity is analyzed. Firstly, analytical results are provided according to the analytical expressions of the capacities. Next, a numerical analysis is presented by applying the real values on the parameters of the obtained capacities and then analyzing their corresponding simulations.

1. *Analytical analysis*

The analytical expressions of the obtained ergodic capacities C_{cell}, C_{D2D} and C_g allow to evaluate the system parameters influence on the global and broadcast received data rates in particular the cellular and D2D transmission powers and the distance between D2D links, CUEs and the BS. As seen in (19), the global capacity of the hybrid model is composed of two functions with different forms. These two functions depend on the D2D and cellular transmission powers and on the attenuation path loss therefore on the distance between transmitters and receivers of the two networks. In (19), the transmission power ratios β_1 and β_2 exist with contradictory manner in the two capacities equation. This affects the global capacity which is the sum of two contrary variations. This interpretation means that the analytical derivation is not sufficient to have an idea on C_g variation. Therefore, because of the complexity of C_g form, the parameter values are needed to evaluate the transmission power variations effect on the global capacity.

2. ***Numerical analysis***

In this section, we will analyse the derived capacity expression in extensive simulations scenario in order to trace the behaviour of D2D underlaying cellular networks. However, this is hard to realize in the analytical approach. Looking into (19), we notice the parameters $\beta_1, \beta_2, A_1, A_2$ and A_3 are function of the path-loss and power transmissions. Path-loss variables, i.e. l_{d1}, l_{d2} l_c, l_k, $l_d$and l_b are given to the simple model ($l = 1/d^{\alpha}$), with α is the path-loss exponent equal to 3. The BS radius is 500 m. The bandwidth of the network is normalized. The BS and D2D TXs can transmit at a maximum of 1.4 W and 0.1995 W respectively.

Figure 2.3 shows the deployment of the simple scenario adopted in this section.

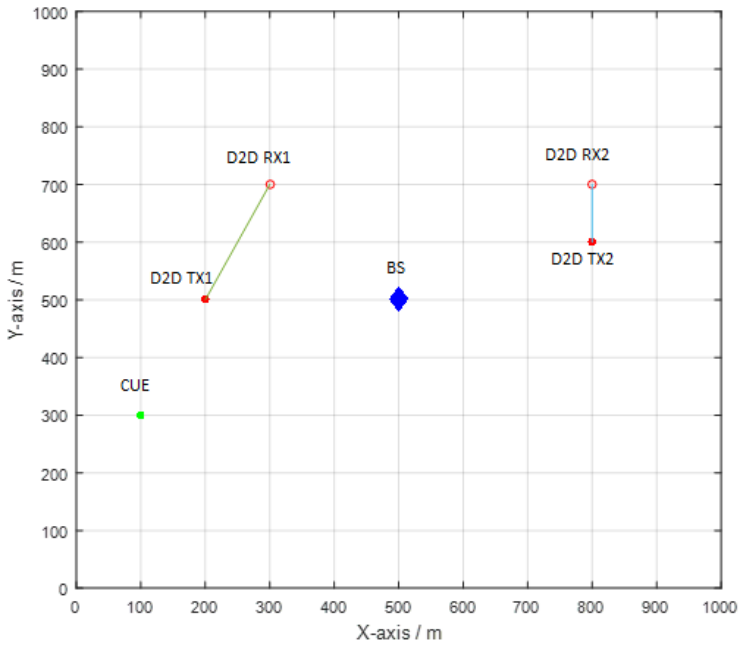

Figure 2.3 Scenario deployment of a BS with a single CUE and couple D2D pair

Applying the parameter values on the simulations, four figures are drawn. The first three figures show the variation of the system capacities in function of the transmission

powers ratio parameters, and the fourth figure shows their variation w.r.t to the power ratio P_d/P_b while fixing the distance parameters.

Firstly, Figure 2.4shows the behavior of the global capacity w.r.t. the cellular and DTXs power ratio parameters, i.e. β_1 and β_2. From this figure, it can be immediately seen that the global capacity is not a convex function of $\beta_1$or β_2. Moreover, the maximum data rate would be obtained for a non-operational D2D system, which would not be desirable.

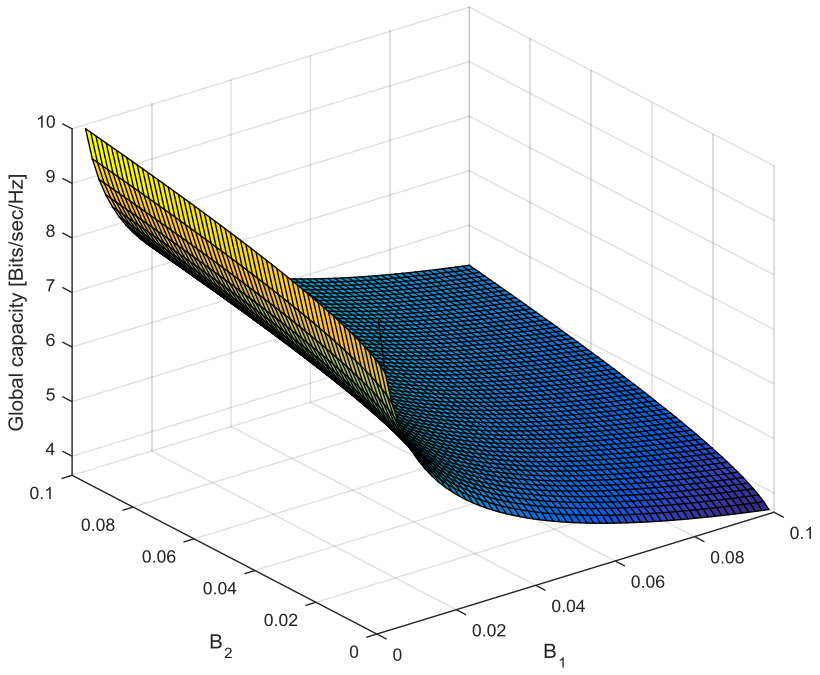

Figure 2.4 Global capacity (bits/sec/hz) as a function of the power ratio parameters β_1 and β_2.

Secondly, the two curves in Figure 2.5 show the behavior of the D2D capacity and cellular capacity w.r.t β_1 and β_2. Clearly in (a), we can observe the property of the curve and can be identified as concave while (b) as convex, although it is indirectly associated with the power transmitted by the DTXs and BS. To that end, Figure 2.6 removes this vagueness and show only the relation of the capacities with the transmitted powers, i.e. P_d/P_b.

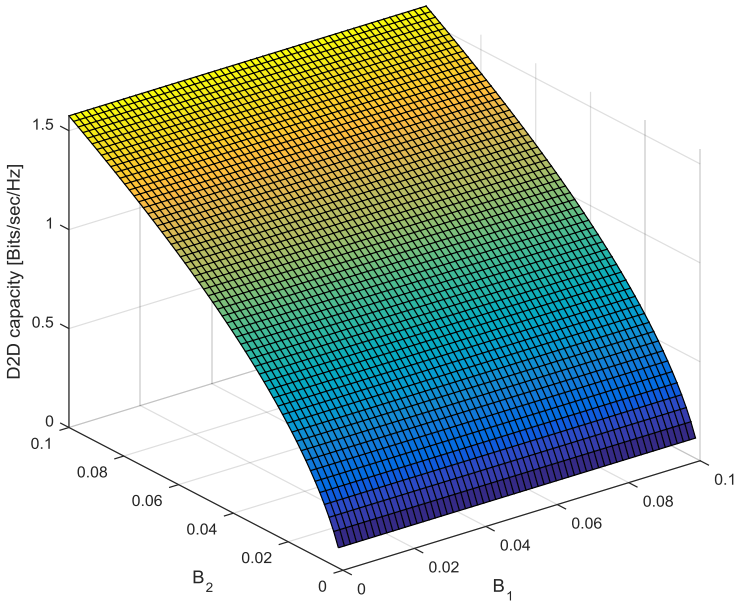

(a)

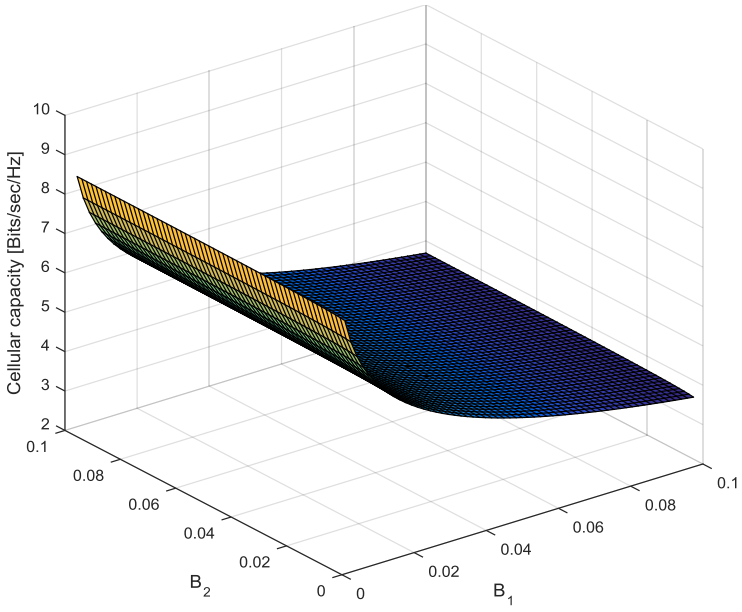

(b)

Figure 2.5 D2D and Cellular capacities (bits/sec/hz) as a function of the power ratio parameters β_1 and β_2.

Figure 2.6 verifies the convexity of the first term and the concavity of the second in equation (19) in term of the power ratio P_d/P_b. As shown in Figure 2.6, the global capacity is maximized at two points, when the power ratio is at 0 or ∞. In other words, one of the systems has to be switched off in order to maximize the global capacity. This convex concave property of the global capacity expression is very

important as it allows specifying the solution of the power optimization problem of both systems.

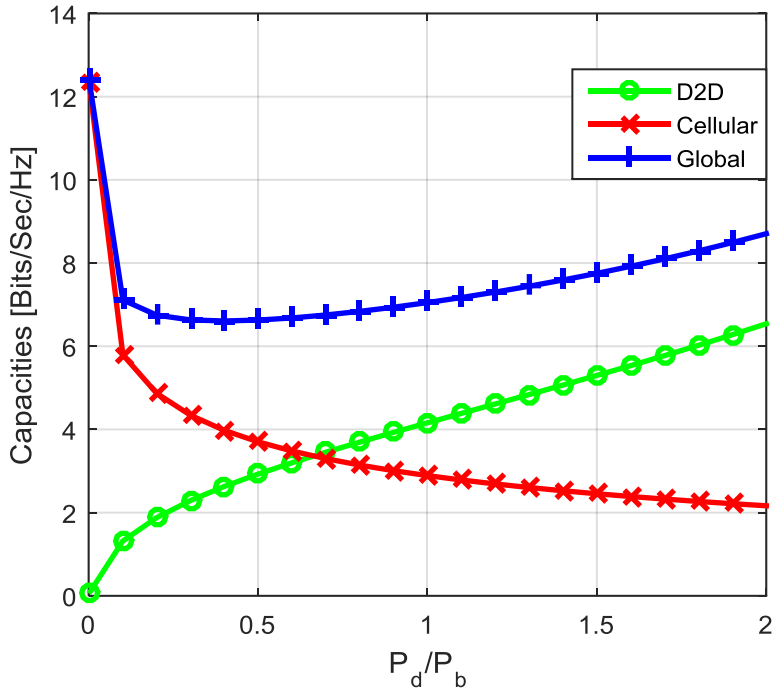

Figure 2.6 Global, Cellular and D2D capacities in terms of the power ratio P_d/P_b

Figure 2.6 also gives us other insights. Let us for example, consider a capacity requirement threshold, seen as a QoS metric, equal to 2 [b/s/Hz]. Clearly the D2D achieves this requirement whenever the power ratio P_d/P_b is higher than 0.25, while on the other hand, the mobile capacity will violate the requirement at power ratio values greater than 2.5. Thus P_d/P_b should be confined between 0.25 and 2.5 to meet the QoS conditions. This indicates the importance of selecting an appropriate QoS threshold which will affect directly the behavior of our optimization.

3. ***CDF and CCDF analysis***

This section derives the CDF/CCDF for the cellular system and discusses the behavior of the analytical results based on the derived expressions of the probability density function. Here we will be assuming the D2D are transmitting with unified power, i.e. the maximum transmitting power of 0.1995 W.

To calculate the CDF and the CCDF of the SIRs for the cellular user, we integrate the density function $p_{\tilde{\gamma}_c}(s)$ of that user as follows:

$$F_{\tilde{\gamma}_c}(s) = \int_{-\infty}^{s} p_{\tilde{\gamma}_c}(s)\, ds$$

$$= \int_{-\infty}^{s} P_b l_c \left[\prod_{i=1}^{N} \frac{1}{P_d l_i}\right] \sum_{j=1}^{N} \frac{\left(P_d l_j\right)^2}{\prod_{\substack{k\neq j \\ k=1}}^{N} \left(\frac{1}{P_d l_k} - \frac{1}{P l_j}\right) \left(P_d l_j s + P_b l_c\right)^2} ds$$

$$= P_b l_c \times \left[\prod_{i=1}^{N} \frac{1}{P_d l_i}\right] \times \sum_{j=1}^{N} \left[\frac{\left(P_d l_j\right)^2}{\prod_{\substack{k\neq j \\ k=1}}^{N} \left(\frac{1}{P_d l_k} - \frac{1}{P_d l_j}\right)} \times \int_{0}^{s} \frac{1}{\left(P_d l_j s + P_b l_c\right)^2} ds\right] \qquad (20)$$

$$= P_b l_c \times \left[\prod_{i=1}^{N} \frac{1}{P_d l_i}\right] \times$$

$$\sum_{j=1}^{N} \left[\frac{\left(P_d l_j\right)^2}{\prod_{\substack{k\neq j \\ k=1}}^{N} \left(\frac{1}{P_d l_k} - \frac{1}{P l_{d_j}}\right)} \times \left(\frac{-1}{P_D l_j \left(P_d l_j s + P_b l_c\right)} + \frac{1}{P_d l_j (P_b l_c)}\right)\right]$$

The CCDF on the other hand is obtained as:

$$\overline{F}_{\tilde{\gamma}_c}(s) = P(X > s) = \int_{s}^{\infty} p_{\tilde{\gamma}_c}(s)\, ds = 1 - F_{\tilde{\gamma}_c}(s) \tag{21}$$

The results in Figure 2.7 show the complementary CDF of the cellular user in a hybrid cellular and D2D system. Specifically it shows the probability that the cellular user will experience SIR (in magnitude) which is higher than a given threshold SIR for different values of N and BS transmit power. For example, assuming N=1 (which is the number of D2D links on the same resources) and BS transmit power pf 10.17 Watts, then the probability that the user will experience SIR higher than 610.2 is 0.6749. Notice that for the same N, as the BS transmit power increases, the probability will also increase which is as expected.

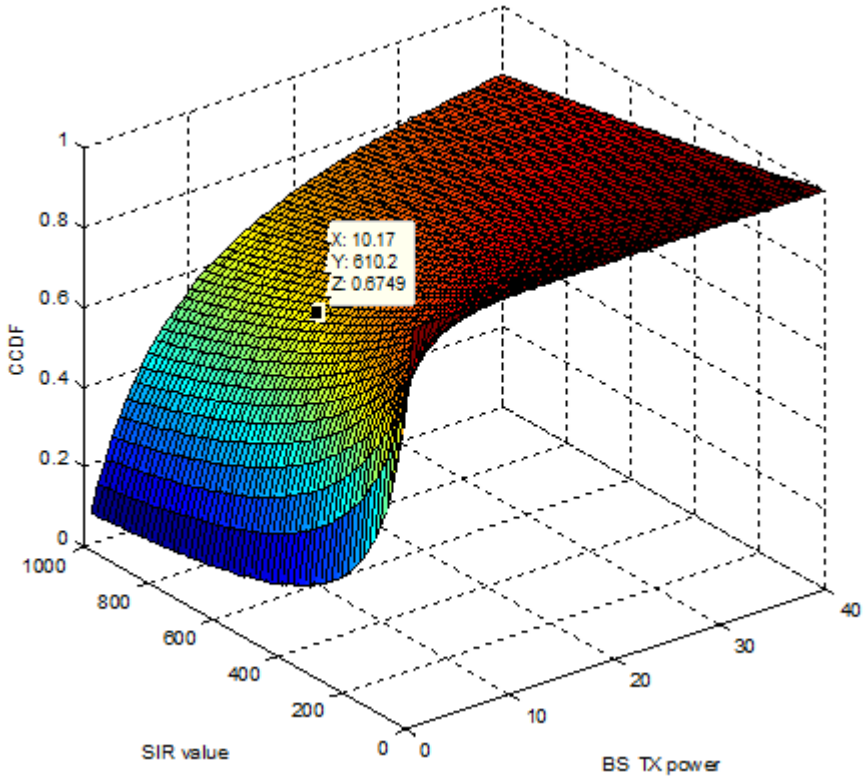

Figure 2.7 The CCDF of the CUE with varying BS TX power and SIR value and with a single D2D pair

Now let's increase the number of D2D links (N) and observe the results:

Assuming N=2, and for the same BS transmit power of 10.17, we notice in Figure 2.8 the probability for SIRs higher than 610.2 is now 0.2998, which is much lower than what it was when the case of N=1.

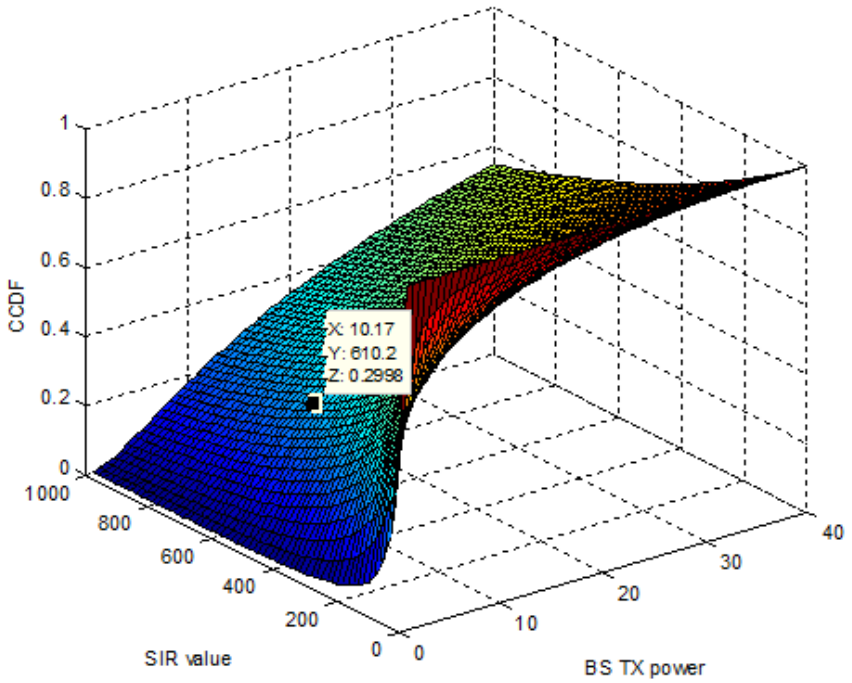

Figure 2.8 The CCDF of the CUE with varying BS TX power and SIR value and with 2 D2D pairs

As a result, we conclude that as N increases, the cellular user will experience more interference in the downlink and thus the CCDF will decrease for the same BS transmit power and target SIR.

Table 2.1 shows the CCDF for different values of N for the same transmitting BS power and SIR values:

Number of D2D pairs (N)	CCDF value
1	0.6749
2	0.2998
3	0.07457
4	0.01048

Table 2.1 CCDF values for different N

CHAPTER III

OPTIMIZATION OF THE GLOBAL ERGODIC CAPACITY

The purpose of this chapter is to improve the performance of coexisting D2D and cellular systems. The intended improvement is to maximize the ergodic capacity of the systems or at least reach a convergence point where the QoS constraints are satisfied. This optimization process targets the special case that was investigated in section C of chapter II, i.e. the case of a single CUE and multiple D2D links. We could easily assume that these D2D links present the maximum interference levels on the CUEs. This assumption made due to the complexity of the expressions in crowded and dense scenarios. The crowded situation will be studied in the next chapter as multiple CUEs coexist with multiple D2D links. We will be using the already derived capacity expressions for our maximization process in terms of power allocation of an objective function given as the sum of D2D and cellular capacities. The latter is composed of a convex and concave parts. As seen in equation (19), the expression depend on the ratio of the transmission power parameters and not on each solely, so it is best to jointly maximize the ratio of the power parameters. The CCCP is applied to the maximization problem under QoS constraints in order to obtain the optimal functioning point.

A. Optimization problem

In order to maximize the global ergodic capacity for the previously defined scenario, a maximization problem must be solved as detailed below. Firstly, the objective function is formulated. Secondly, the maximization problem is presented.

1. *Problem formulation*

Our target is to jointly maximize the global capacity under QoS constraints. Then, our problem is formulated as follows:

$$\begin{aligned} &\underbrace{max}_{\beta_1,\beta_2} \; C_g\,(\beta_1,\beta_2) \\ s.t. \quad &C_{cell}(\beta_1,\beta_2) \;\geq\; \alpha_{cell} \\ &C_{D2D}(\beta_1,\beta_2) \;\geq\; \alpha_{D2D} \end{aligned} \tag{22}$$

α_{cell} and α_{D2D} are two thresholds inserted in the optimization process to satisfy the required QoS constraint. Then the Lagrangian of this problem can be written as

$$\begin{aligned} L\,(\beta_1,\beta_2,\lambda,\nu) = (1+\lambda)C_{cell}(\beta_1,\beta_2) + \\ (1+\nu)C_{D2D}(\beta_1,\beta_2) - \lambda C_{cell\_th} - \nu C_{D2D\_th} \end{aligned} \tag{23}$$

where $\lambda,\nu \geq 0$, are the Lagrangian multipliers associated to the constraints in (22). For tractability and to simplify the optimization process, we consider the power ratio $x = P_d/P_b$ as the metric to be optimized in our work. It is captured in β_1 and β_2 parameters. Moreover, the maximization problem is shown to be a convex-concave formulation based on the analysis in section D of chapter II, hence we propose to use the CCCP to find the optimal solution.

2. ***CCCP background and Procedure***

a. Application conditions

The function $f_1(x)$, to be optimized with CCCP procedure, should have a bounded Hessian $\partial f_1(x)/\partial x \partial x$ and could be always decomposed into the sum of a convex function and a concave function. When a convex function $f(x)$ has positive definite Hessian with eigenvalues bounded below by $\epsilon_{CCCP} > 0$, then there exists a positive constant λ such that the Hessian of $f(x) + \lambda g(x)$ is positive definite and hence $f(x) + \lambda g(x)$ is convex. Hence $f(x)$ can be expressed as the sum of a convex part, $f(x) + \lambda g(x)$, and a concave part $-\lambda g(x)$ [17].

b. CCCP convergence

The function $f(x)$ (bounded below), to be optimized, is with the form:

$$f(x) = f_{cave}(x) + f_{vex}(x) \tag{24}$$

with $f_{vex}(x)$ and $f_{cave}(x)$ are respectively convex and concave functions of x.

Then the discrete iterative CCCP algorithm $\vec{x}^t \rightarrow \vec{x}^{t+1}$ given by:

$$f_{vex}(\vec{x}^{t+1}) = -\vec{\nabla} f_{cave}(\vec{x}^t) \tag{25}$$

is guaranteed to monotonically decrease $f(x)$ as a function of time and hence to converge to a minimum or saddle point of $f(x)$.

c. CCCP algorithm

A CCCP algorithm is illustrated for Convex minus Convex. Figure 3.1 represents an example of $f(x)$. If the problem is to minimize the function in the Left

Panel in Figure 3.1, it must decompose it (Right curves) into a convex part (top curve) minus a convex term (bottom curve), which means $f(x) = f_{vex}(x) - \left(-f_{cave}(x)\right)$. The algorithm iterates by matching points on the two curves which have the same tangent vectors. The algorithm rapidly converges to the solution. The convexity of $f_{t+1}\ (\vec{x})$ implies that there is a unique minimum $\vec{x}^{t+1} = arg\ \min_{x} f_{t+1}(\vec{x})$. This means that an inner loop is needed to calculate $\vec{x}^{t+1}$ then we can use standard techniques such as conjugate gradient descent and a lot of other existing methods according to the problem case.

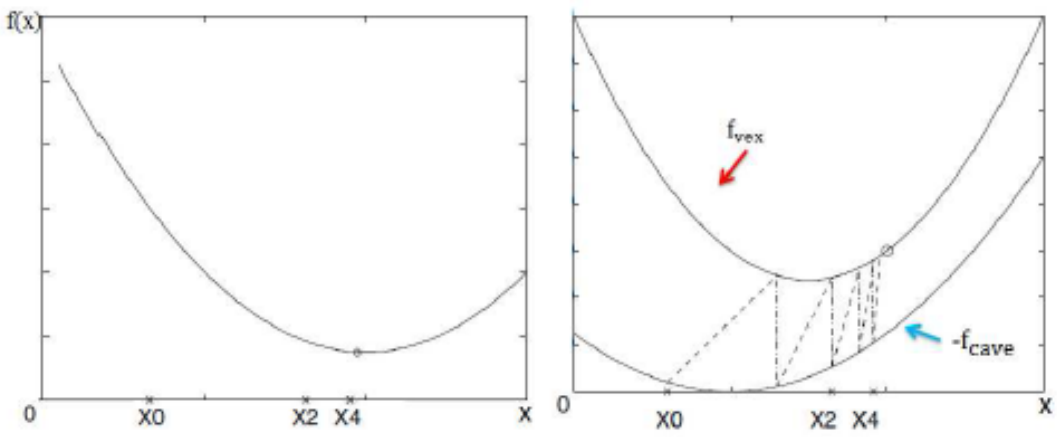

Figure 3.1 The function to minimize is a sum of convex and (-convex) functions [17]

3. ***Problem optimization***

By analogy in equation (23), the convex term in L is $(1+\lambda)C_{cell}(\beta_1,\beta_2) - C_{cell\_th}$, and the concave term is $(1+\nu)C_{D2D}(\beta_1,\beta_2) - \nu C_{D2D\_th}$.

Then the procedure will become:

$$\nabla L_{vex}(x^{t+1}) = -\nabla L_{cave}(x^{t}) \tag{26}$$

By applying (26) in (23), we get the following:

$$\nabla C_{cell}(x^{t+1}) = -\frac{1+\nu}{1+\lambda}\nabla C_{D2D}(x^{t}) \tag{27}$$

Hence, an iterative algorithm for the implementation of CCCP is proposed based on (27).

This algorithm, given below, tries to obtain the optimal power ratio x^* meeting QoS threshold as seen in the loop at step 5, while the loops at steps 8 and 17 will calculate the optimal Lagrangain multipliers for a certain x.

Algorithm CCCP for global capacity optimization [14].

Required: $\alpha_{cell}, \alpha_{D2D} > 0$,

Outcome: Return the optimal power ratio x^* between D2D and LTE

1. Initialize $\epsilon > 0$, λ_{min}, λ_{max}, υ_{min}, $\upsilon_{max}$and x^0
2. $\lambda \leftarrow (\lambda_{min} + \lambda_{max})/2$, $\upsilon \leftarrow (\upsilon_{min} + \upsilon_{max})/2$
3. Update x^{t+1} with (27) $x_1 \leftarrow x^{t+1}$
4. Update both $C_{cell}(x^{t+1})$ and $C_{D2D}(x^{t+1})$
5. **while** $|x^{t+1} - x^t| > \epsilon$ or $C_{cell} < \alpha_{cell}$ or $C_{D2D} < \alpha_{D2D}$ **do**
6. $x^t \leftarrow x_1$ and update x^{t+1} with (27)
7. Update $C_{cell}(x^{t+1})$ and $C_{D2D}(x^{t+1})$
8. **while** $\lambda_{max} - \lambda_{min} > \epsilon$ **do**
9. **if** $C_{cell} < C_{cell\_th}$ **then**
10. $\lambda_{max} \leftarrow \lambda$
11. **else**
12. $\lambda_{min} \leftarrow \lambda$
13. **end if**
14. $\lambda \leftarrow (\lambda_{min} + \lambda_{max})/2$
15. $x^t \leftarrow x_1$ and update x^{t+1}
16. Update $C_{cell}(x^{t+1})$ and $C_{D2D}(x^{t+1})$
17. **while** $\upsilon_{max} - \upsilon_{min} > \epsilon$ **do**
18. **if** $C_{D2D} < C_{D2D\_th}$ **then**
19. $\upsilon_{max} \leftarrow \upsilon$
20. **else**
21. $\upsilon_{min} \leftarrow \upsilon$
22. **end if**
23. $\upsilon \leftarrow (\upsilon_{min} + \upsilon_{\max})/2$
24. $x^t \leftarrow x_1$ and update x^{t+1}
25. Update $C_{cell}(x^{t+1})$ and $C_{D2D}(x^{t+1})$
26. end while
27. end while
28. end while
29. $x^* \leftarrow x^{t+1}$

B. Simulation and Analysis

In this section, we provide simulation results obtained by the CCCP algorithm. Table 3.1 summarizes the parameters used in our simulations. The distance between D2D TX1 and LTE RX is a simulation parameter ranging from 50 m to 2000 m. Figure 3.2 shows the optimal transmit power ratio x^* for the range specified of D2D TX1- LTE RX separation in meters, and for QoS constraints of $\alpha_{cell} = 5$ bits/s/Hz, $\alpha_{D2D} = 1$ bits/s/Hz. As can be seen in this figure, as distance increases, x^* also increases. Indeed, this behavior is expected, since with larger separations, the D2D can transmit with higher power to maintain its capacity threshold. At larger distances, the optimal ratio seems to saturate.

Parameter	Default Value
BS – LTE RX distance (m)	100
BS – D2D RXs distances (m)	1000, 500
Cross D2D links separation (m)	1500
D2D links separations (m)	120, 100
D2D TXs – LTE RX distances (m)	50 →2000
Path-loss exponent for both systems	3
Realizations at each x	100

Table 3.1 Simulation parameters for the CCCP algorithm

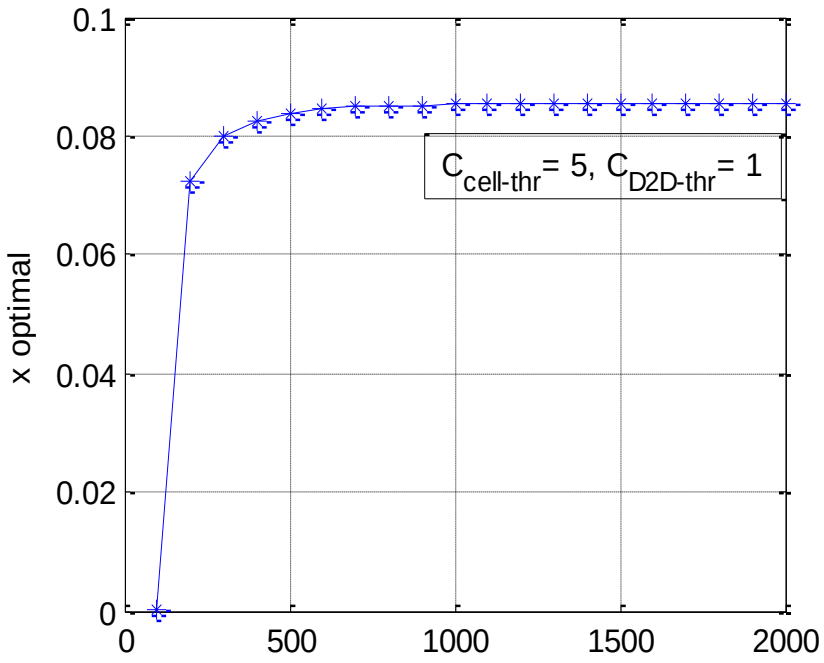

Figure 3.2 x^* as a function of D2D TX1 - LTE RX distance (m)

In addition, the relation of the optimal power ratio with the capacities is given in Figure 3.3 where at a power ratio x tends to 0, the D2D is switched off while the cellular system is at maximum capacity. Then, as x^* increases, the cellular capacity will decrease and as a result, the D2D will have higher capacity. By inspecting the global capacity, we find it to be minimized when both systems satisfy the QoS constraints, and maximized whenever one system is dominant over the other. Hence, for fair operation among both systems, the global capacity is at minimum as shown in Figure 2.6.

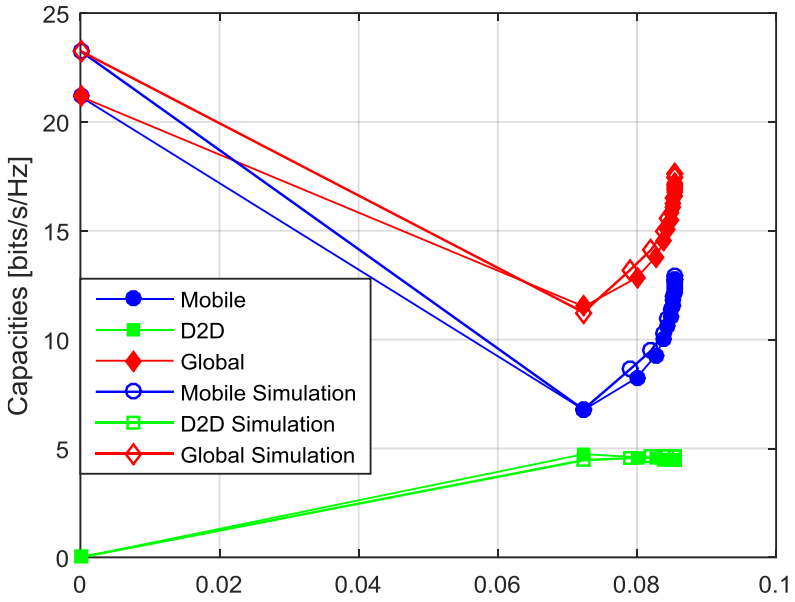

Figure 3.3 Mobile and D2D Capacities as function of x^*

The results of our algorithm can be verified in by applying the optimal power ratio x^* resulted from the CCCP algorithm into a simulation scenario with the same setup. As can be seen in Figure 3.3, the results we obtained match those of the algorithm, and this shows the robustness of our algorithm.

Figure 3.4 shows the variation of the capacities w.r.t. the D2D TX1 - LTE RX distance. Indeed as this separation increases, we expect less interference on the DL resources, resulting in higher capacity for the LTE user. On the other hand, since the D2D only assumed operational on the DL, no interference should come from the LTE user, so the capacity remains relatively stable. In other words, as long as the cellular separation is large enough, the D2D capacity will not be affected by the cellular interference, as expected.

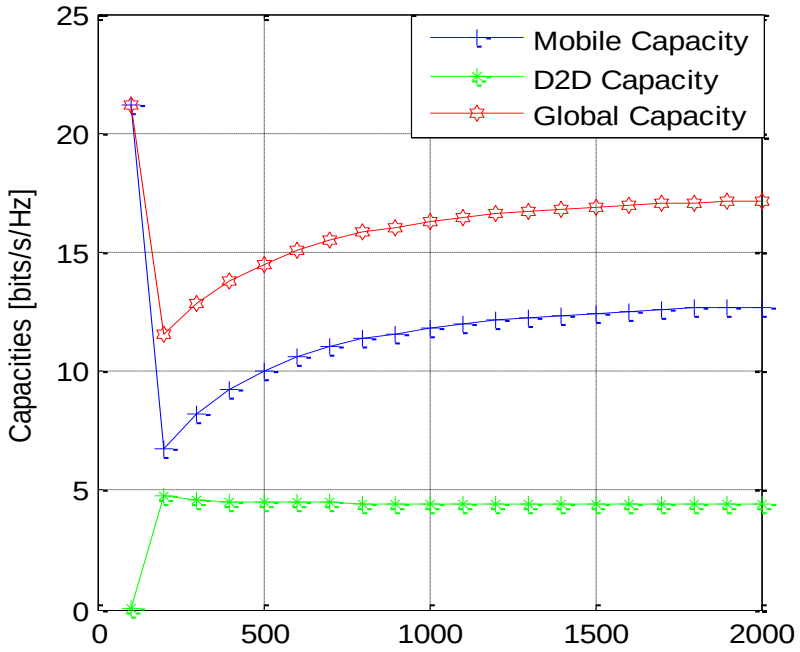

Figure 3.4 Mobile and D2D Capacities as function of D2D TX1 - LTE RX distance

Finally, it is worth mentioning that the power allocation is obtained by maximization of the joint capacity which does not necessarily mean a maximization of each capacity. Hence, for instance, the cellular capacity might decrease even when the D2D TX1 - LTE RX distance increases while the D2D capacity increases.

CHAPTER IV

CAPACITY ANALYSIS AND OPTIMIZATION USING GEO-STATISTICAL MODELING

Spatial statistics constitute a powerful tool utilized in the solution of a broad spectrum of problems in different fields, ranging from sociology or medicine to engineering and technology. The particular field of wireless communications has also made use of different techniques drawn from this field [17], [18].

In this chapter, we develop a solution for the D2D power allocation problem in dense D2D underlaying cellular network topology. The analytical derivations for such model becomes complex and difficult to analyze as the number of devices increase. Therefore, we refer to the geostatistical modeling for radio environment predictions, explicitly by observing the spatial coverage cross-correlation between the BS and the D2D links in the DL spectrum, then propose an iterative algorithm based on the construction of SINR regions or tessellations to give better insights for the power allocation. The resulting information are incorporated in Matlab tool CVX, that is used for solving convex and concave problems; where it gives the optimal D2D power allocations, maximizing the global capacity of the network.

A. Geostatistics background

Geostatistics is described as a spatial statistical tool that can be employed in any practical problem where predictions of a random variable are needed in a 1D, 2D or 3D application. The basic theoretical framework of geostatistics was developed in the early 1950's mainly for mining purposes to estimate ore reserves. Today geostatistics is widely recognized as a tool for accurate spatial estimation [19]. The first attempt to demonstrate that geostatistical techniques can be effectively and pragmatically applied in the domain of signal strength estimation is presented in [20], where they consider these methods powerful and statistically rigorous and encourage researchers to further investigate this concept when approaching the problem of empirical radio environment mapping. There is no work done in the literature as far as we know on the application of geostatistical modelling into the coexistence of D2D and cellular networks, hence we propose to investigate this application to the incorporation of the power optimization problem. Among others, Kriging is a popular geostatistical method that has been proposed for use in the domain of signal strength estimation [21]. We will discuss this technique further in the following section.

1. *Kriging background*

In 1951 a South African Mining Engineer, D.G. Krige, published a seminal paper in the journal of the Chemical, Metallurgical and Mining Society of South Africa, where he pursued a statistical exploration of the conditional biases in ore block valuations. This formed the basis of the interpolation method known today as kriging [22]. The French mathematician G. Matheron, who is known for laying the

foundation of geostatistics, adapted and formalized the work of Krige in 1963 [24]. Kriging is defined as an optimal interpolation method based on regression against observed values of surrounding data points, weighted according to spatial covariance values [22].

Kriging can be divided into three main types: simple kriging, ordinary kriging, and universal kriging. In our work we will be adopting the ordinary kriging since it is the most suitable for our scenario.

Kriging forms weights from surrounding measured values to predict values at unmeasured locations. As with interpolation techniques, the closest measured values have the most influence. However, the kriging weights for the surrounding measured points are more sophisticated than those of these techniques. Inverse Distance Weighting (IDW) for example, uses a simple algorithm based on distance, but kriging weights come from a semivariogram that was developed by looking at the spatial structure of the data. To create a continuous surface or map of the phenomenon, predictions are made for locations in the study area based on the semivariogram and the spatial arrangement of measured values that are nearby [25].

B. System model and Fields evaluation

In this section, we develop the system model and apply the ordinary kriging to generate a prediction of the coverage fields for both the cellular and D2D systems. Specifically we obtain the SINR predictions in unmeasured locations in the network where no working devices exist. Then we discuss the resulting maps and investigate the cross-correlation of the both network.

1. ***System model***

We consider a basic scenario where D2D UEs coexist with CUEs in the same coverage area of the Macro BS. The BS uses the DL LTE band to deliver important control signals to cell associated users, where all CUEs share the resources orthogonally, and we assume that D2D users reuse the DL resources. So CUEs do not cause interference between themselves, but D2D UEs will interfere with nearby cellular transmissions. The general model for resource sharing is shown in Figure 4.1, with multiple D2D and cellular links, where solid links represents an ongoing transmission and red dashed link represents an interference signal

In our model, we assume that the mobile users are spatially distributed according to a PPP with density λ. Figure 4.2 shows a deployment scenario model. The D2D links are represented, with the filled circles being the TXs and the empty ones being the RXs. If a device is associated with a BS for regular cellular communication, it is represented by a star sign. Note that for convenience, we removed the cellular links for the sake of clarification. Table 4.1 shows the simulation network parameters adopted in this section.

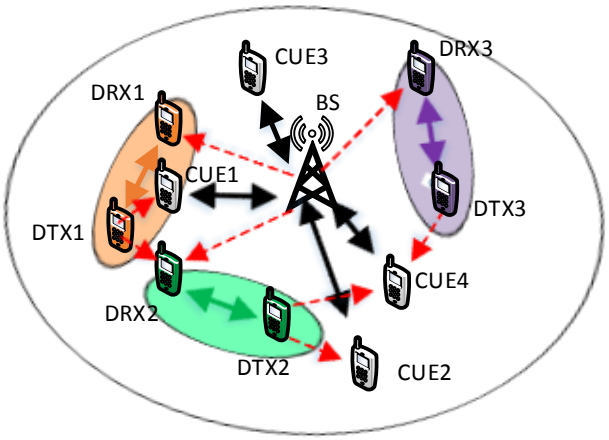

Figure 4.1 D2D and cellular systems sharing resources

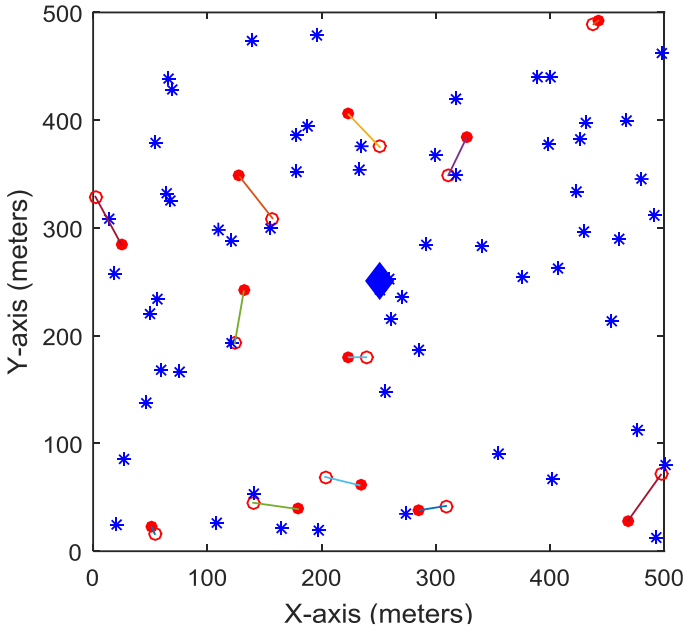

Figure 4.2 scenario deployment. Users are distributed as PPPs with density λ=100. D2D links attachment are based on max distance threshold

Parameter	Default Value
BS coverage area (m^2)	500
Users density λ	100
BS transmit power (Watts)	40
UE transmit power (dBm)	23
Channel realizations	1000
Path-loss exponent	3
Power level thermal noise (dBm/Hz)	-112.2391
Max feasible distance between a D2D link (m)	50

Table 4.1 Network Simulation Parameters

2. ***Coverage fields***

As mentioned before, Kriging uses the distances and the spatial arrangement of the users or devices to calculate the spatial correlation or the semi-variogram γ [18], [19]. This technique, unlike most deterministic interpolation approaches, assumes that the measurements are random processes with some trait of dependence between them. Moreover, it can generate prediction surfaces and provide a decent level

of accuracy for these predictions. Thus, its advantage over deterministic models appear in being less complex to establish a prediction for the coverage fields in environments where input parameters are hard to obtain. For instance, for a cellular BS, it would be hard to obtain the power transmitted by each D2D, hence an estimation of this power is necessary for the optimization purposes.

The empirical correlation, widely known as semi-variogram, is calculated by:

$$\gamma(x,y) = 0.5 \times E\left[\left(Z(x) - Z(y)\right)^2\right] \tag{28}$$

where (x,y) are two different locations, and Z represents the SINR for D2D links at these locations. Using the SINR values of D2D receivers, we can develop the coverage map in a specified range. This map serves as an important factor in devising an algorithm to enhance system throughout and sum-rate capacity [18].

a. Coverage maps interpretation

The estimation of SINR coverage maps is shown in Figure 4.3. It is noted that in our case study, we did not consider the scheduling phase, which means the devices are only able to measure and report on their interference levels, at their location. As expected, we notice in Figure 4.3 (a), a degradation in the received signal quality for D2D communication near the location of the BS which gets improved when the links are away from it. Contrariwise, the SINR level for CUEs is at its best near the BS and starts to fade with distance due to path-loss effect, not to mention the minima are caused by the interfering D2D TXs which are near that location.

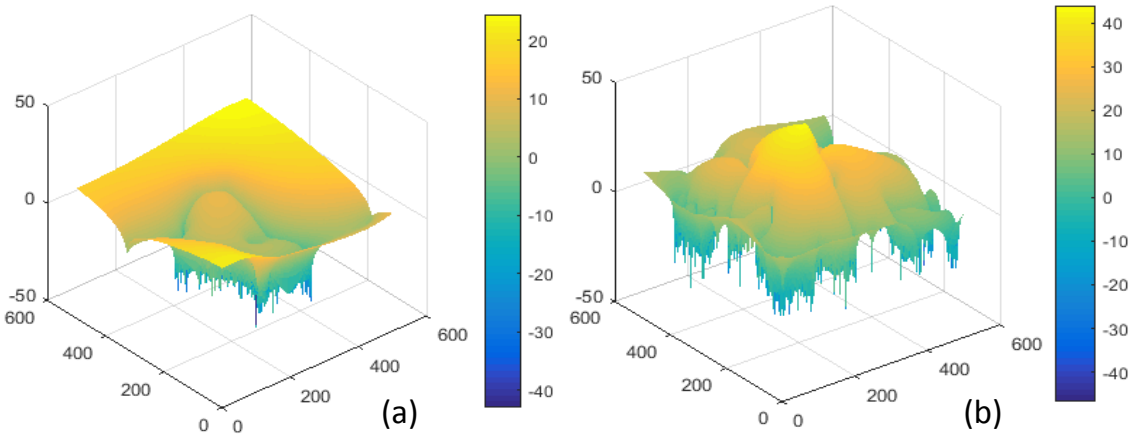

Figure 4.3 Coverage field estimation using OKE exponential model fitting. (a) D2D SINR field. (b) Cellular SINR field

b. Cross-Correlation of the fields

Figure 4.4 shows the normalized spatial cross-correlation of the D2D SINRs compared to cellular SINRs of the network, which was generated using the built-in MATLAB function *normxcorr2*. The figure exhibits minima around the BS position, which is intuitive because the BS will highly interfere with proximate D2D users on the downlink while CUEs having the maximum received power. The negative correlation depicts locations of high interference seen in the center and edges, otherwise the SINRs correlations become independent.

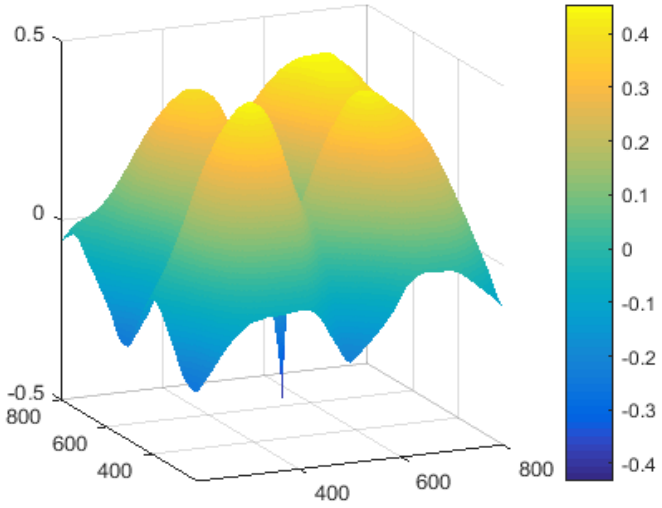

Figure 4.4 Cross-correlation of D2D and Cellular SINR fields

This figure is a very important result of the OKE tool as it allows the utilization of the coverage map in resource and power allocation for both D2D and cellular UEs. Indeed, due to the high cross-correlation factor and starting with the cellular coverage maps obtained through OKE, the scheduler could estimate the interference level nearby the D2D links and could allocate the resources accordingly. In other words, one can exploit the spatial correlation rather than the optimization of the ergodic capacities given in the previous chapters, to determine how to optimize the network by some interference management techniques. The interest of the coverage maps becomes more significant when the number of D2D links increases as it would be unmanageable to find a close-form expression of the global capacity optimization problem similar to equation (19) in chapter II.

To illustrate the importance of using geostatistics, consider Figure 4.5, where the behavior of the mean ergodic capacities of the D2D and cellular systems for the considered model is interpreted. As can be seen in the figure, when the BS is idle, the capacity of the D2D links is maximum, as expected. Indeed, the only interference is

from adjacent D2D links. The higher the transmit power intensity of the BS is, the worse the capacity of the D2D system is, resulting in poor QoS for these devices. Referring to equations (17) and (18), we can see that the expressions depend on the power ratios of D2D and the BS as well as on the distances included in the path-loss parameters. Hence for fixed power transmissions, the distribution and separation of the devices are the key factors affecting the global capacity. That being said, the use of geostatistical techniques such as ordinary kriging is crucial in order to optimize the network's overall QoS, and also to predict the behavior of the SINR distributions when new users/devices are introduced to the system. Specifically, these new links should be associated considering their contribution in boosting or worsening the overall global capacity based on their locations.

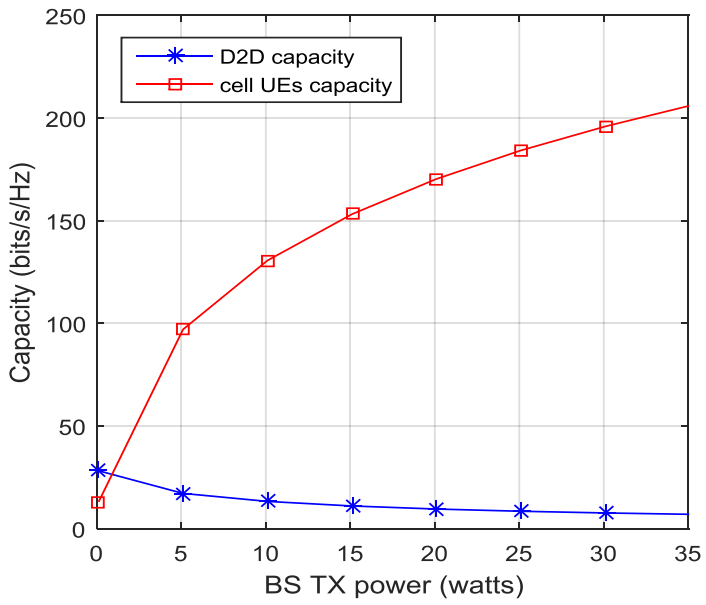

Figure 4.5 Capacity of the hybrid system vs the BS transmit power

C. Optimization Problem

The predicted coverage maps are key inputs for the optimization problem in this section, as they will be incorporated in the objective function to be optimized as will be discussed later. Furthermore, it is noted that this optimization differs from the previous one in its versatility to function over multiple cellular devices and D2D links, which is not feasible with the analytical model derived in chapter II due to the complexity of the expressions for increasing number of devices. Hence, the use of geostatostcial modeling.

1. *SINR Regions*

In our formulation, we propose to divide the coverage map of the D2D network into SINR regions as follow:

1. High SINR region.
2. Medium/fair SINR region.
3. Low SINR region.

In this case, it becomes easier to trace regions of interest as well as the locations that are the most susceptible to interference. In addition, the methodology reduces the simulation time and complexity by gathering SINR ranges instead of working on singular values.

Figure 4.6 illustrates the grouping of the SINR map of the D2D system into 3 main categories. The first category is assumed on the range above SINR values of 10 dB, the second confined between 0 dB and 10 dB, the third below 0 dB.

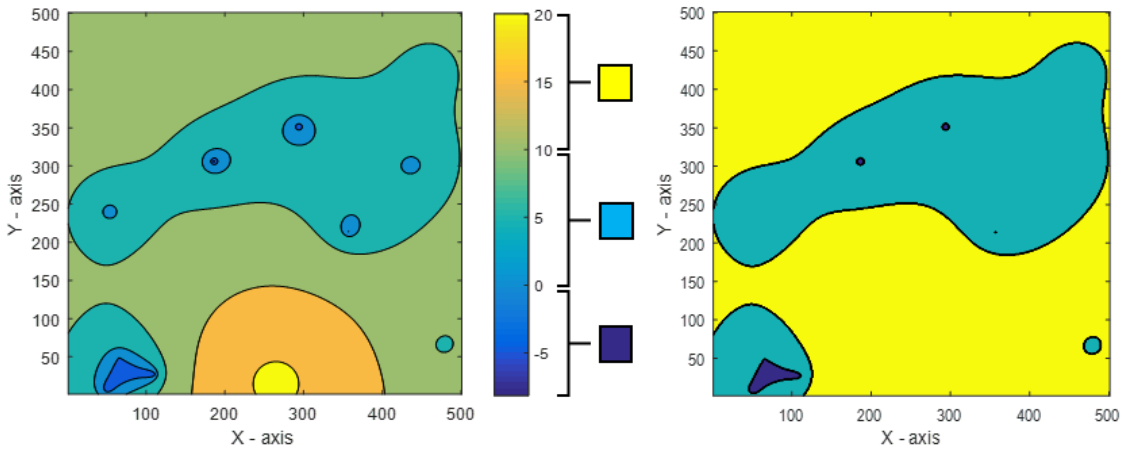

Figure 4.6 SINRs (dB) of the D2D system grouped into 3 categories

Devices located within the same tessellation or region, will be allocated the same TX power corresponding to the optimal power for that region. In addition, we will assume each region having a single D2D link that captures the existence of all pairs in that region. In that sense, and since we only have three SINR ranges, the problem is reduced to finding the three optimal TX powers for each category.

The location of the D2D link is selected to be at the location of the centroid of its tessellation. In geometry, a centroid refers to arithmetic mean position of all the points in a shape or region, consequently, this centroid (if the region is convex) lies in the region's central void.

Figure 4.7 shows the scenario described before and the centroid selection by using image processing functions in MATLAB. The process of finding the centroid location is done separately for each category, then the results are aggregated into a single plot. As can be seen, the yellow spots indicate the regions where the SINR values are within the range of interest, otherwise they are colored purple. When multiple regions exist, then only the most significant one is processed as shown by the red circles. Indeed, this suggests more D2D users are distributed in this region more likely.

Each of the SINR region is defined with a D2D link (TX and RX) separated by the mean distance of all links in the region.

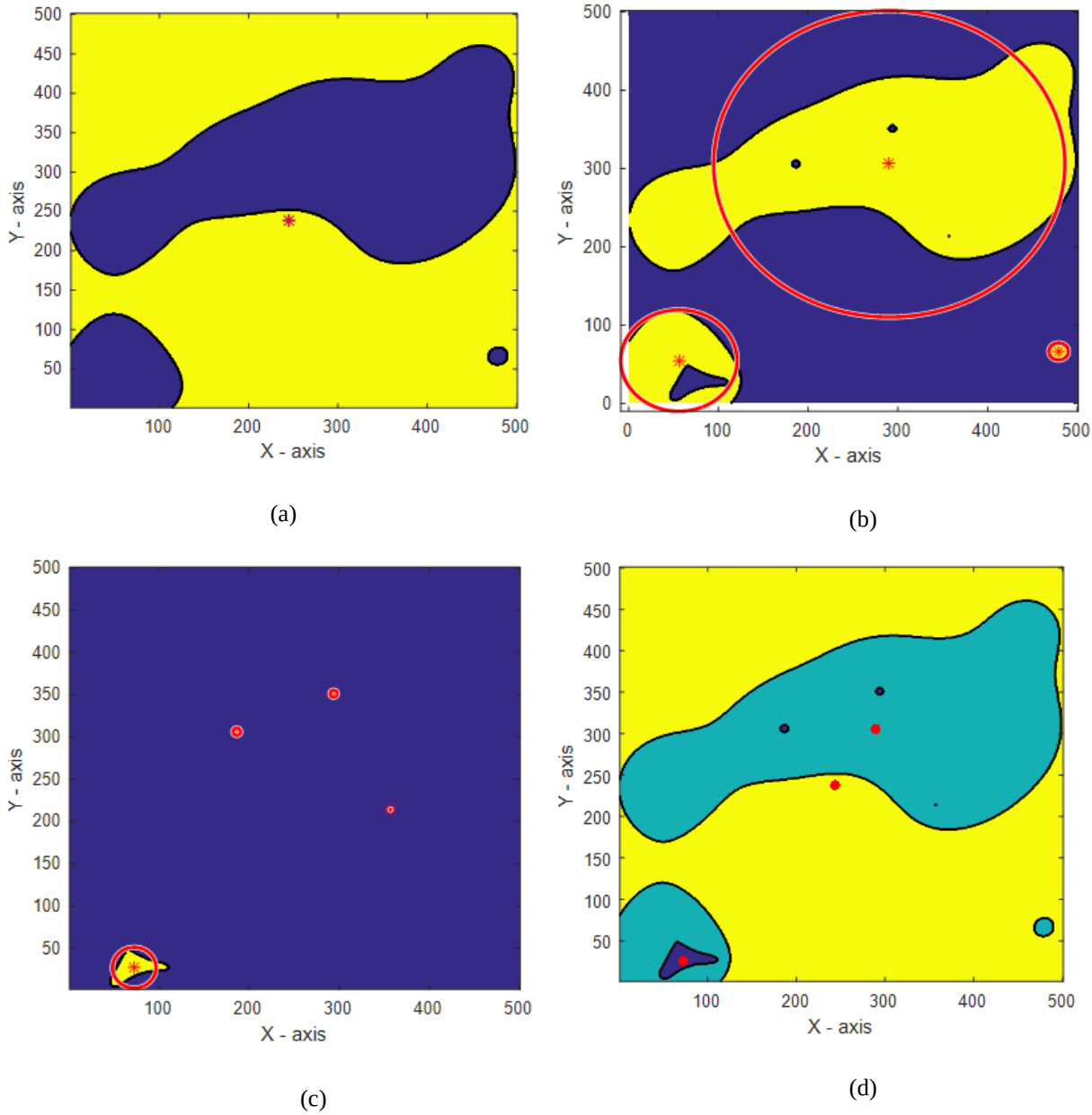

Figure 4.7 Centroid selection representation in the most significant D2D SINR regions. (a) SINR region 1 (b) SINR region 2 (c) SINR region 3 (d) SINR regions combined

2. ***Problem formulation***

In this section, we formulate the optimization problem and present our algorithm that incorporates the previously described approach .The objective of the optimization is to allocate the TX powers to the D2D transmitters which maximizes the capacity of the D2D system while guaranteeing minimum QoS constraints. The process also tries to maintain the SINR of the cellular system above a minimum threshold. It is formulated as follows:

Objective $\quad maximize \ \sum_{i=1}^{M} \log_2(1 + SINR_i)$

Subject to $\quad 0 \leq P_i \leq P_{max}$

$\quad SINR_i \geq \alpha \qquad \forall\, i$

$\quad SINR_j \geq \beta \qquad \forall\, j$

where

$$SINR_i = \frac{P_i r_i |h_i|^2}{I_i + N_0} \tag{29}$$

$$SINR_j = \frac{P_b r_j |h_j|^2}{I_j + N_0} \tag{30}$$

$SINR_i$ is the signal to interference and noise ratio of the i^{th} D2D receivers. $SINR_j$ on the other hand, is the signal to interference and noise ratio of the j^{th} cellular receiver. M is the number of SINR categories (set to 3). P_i is the transmit power of the D2D to be optimized, P_b is the BS transmit power. The path-loss model is considered as $r_i = d_i^{-a}$ where a is the pathloss coefficient and d_i is the distance between the corresponding transmitter and receiver. $|h|^2$ is the channel gain. N_0 is the thermal noise, α is the

minimum required SINR level for the D2D devices and β is the minimum required SINR level for the cellular devices.

I_i is the downlink interference on the i^{th} D2D receiver and is represented by:

$$I_i = \sum_{\substack{j=1 \\ j \neq i}}^{M} P_j r_j |h_j|^2 + P_b r_b |h_b|^2 \tag{31}$$

Since we are considering the devices are sharing DL resources, on each D2D receiver there will be $M - 1$ interfering transmissions as well as the BS transmission.

I_j is the downlink interference on the j^{th} cellular receiver and is represented by:

$$I_j = \sum_{j=1}^{M} P_j r_j |h_j|^2 \tag{32}$$

Having only one D2D link per region, the CUEs experience three interfering signals, indeed, since the D2D link in the center could be interpreted as the average signal strength in that region.

I_i and I_j in our optimization problem are not variable and are known for a given power. They could be easily extracted at any desired location by mathematical manipulation on the SINR maps produced by OKE as in the previous section. So instead of analytically calculating their values, we will be referring to the interference map of each network as can be seen in Figure 4.8. This figure shows the interference on the D2D RXs for the previously described scenario. The Z – axis of this figure represents the value of the interference in magnitude on the D2D RXs that is due to nearby TXs and the BS.

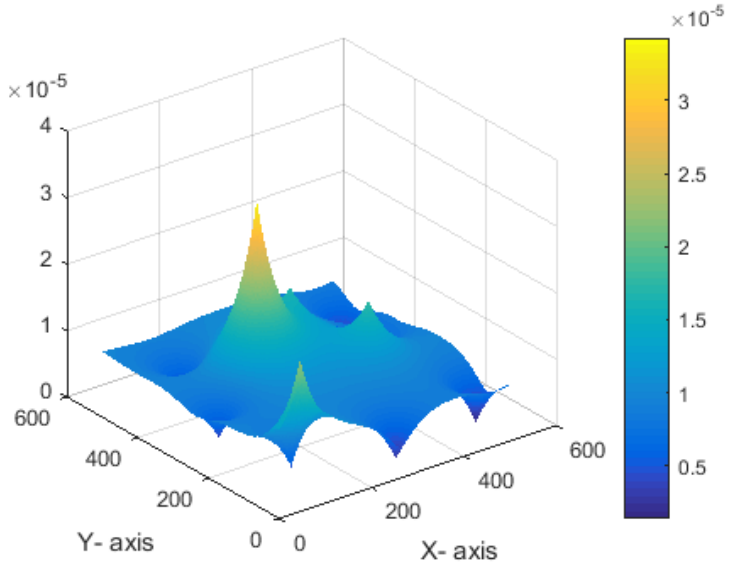

Figure 4.8 The Interference map on the DL D2D RXs

The fact that the capacity of the D2D system is concave w.r.t the transmit powers ratio as seen Figure 2.6, the problem described above can be solved using a convex optimization tool such as CVX which is known for capability with such problems. In addition, an iterative approach is proposed to automate the process of regions construction and centroid selection. The following algorithm tries to solve the formulated problem and returns the optimal power allocations for each region.

Algorithm Power allocation for D2D.

Input: Users with their coordinates and channel knowledge at the BS
Outcome: Return the optimal power allocation vector for D2D at each SINR region

1. Initialize $\alpha, \beta, \epsilon, P, P_{old} > 0$
2. Set initial $P \leftarrow P_{max}$ and calculate the SINRs for the users
3. Apply kriging prediction technique and produce SINR coverage maps for D2D and cellular
4. **while** $|P_{old} - P| > \epsilon$ or $SINR\_cell < \beta$ or $SINR_{d2d} < \alpha$ **do**
5. set $P_{old} \leftarrow P$
6. Construct the SINR regions on the D2D coverage map produced by the kriging prediction tool
7. Extract the location of the centroid in each SINR region and only consider the most significant one for the three regions
8. Calculate the distances with the path-loss and fading coefficient

9. Extract the necessary information of I_i and I_j based on the coordinates of the previous step
10. Begin CVX optimization $\rightarrow P_{optimal\_vec}$
11. Set $P \leftarrow P_{optimal\_vec}$
12. apply the optimal power allocation to the original scenario with each D2D user transmitting with the corresponding allocated power in its region
13. update $SINR_{cell}$, $SINR_{d2d}$
14. Apply kriging prediction technique and produce new SINR coverage maps for D2D and cellular
15. **end while**
16. $P^* \longleftarrow P$

The algorithm returns the optimal power allocation vector of length 3, i.e. the three power values, corresponding to the three SINR regions; which maximizes the objective function and satisfies the QoS constraints. As a result, D2D users in a certain SINR region are allocated with the optimal TX power that the region belongs to in order to maximize the transmission capacity of the network. As an example, should the optimization algorithm yield the following power vector [0.145; 0.09; 0.1995], and assuming that D2D pairs are located in SINR region 2, then the DTXs are bound to transmit with $P = 0.09$ W for an optimal transmission rate.

D. Simulation and Analysis

We did the simulations for a static scenario (no mobility models) where the users are independent and identically distributed. Furthermore, we assume a full buffer model, i.e. a TX is always transmitting at any given time. The simulation parameters are summarized in the following table.

Parameter	Default Value
BS coverage area (m^2)	500
Users density λ	100
BS transmit power (Watts)	5
Realizations	1000
β(dB)	15
α (dB)	10
ϵ	0.001
P_{max} (Watts), $P_{initial}$ (Watts)	0.3, 0.1995
Fading model	Rayleigh

Table 4.2 Simulation parameters for D2D power allocation

Figure 4.9 and 4.10 show the CDF of the SINRs for the D2D and CUEs before and after optimization. The new SINR values for the D2D system are shown to be improved by at least 5 dBs within the range of -10 to 10 dBs. Furthermore, we notice the overall SINRs for the cellular system to be improved on values greater than 4 dBs, otherwise the probabilities remain the same or relatively lower on some values.

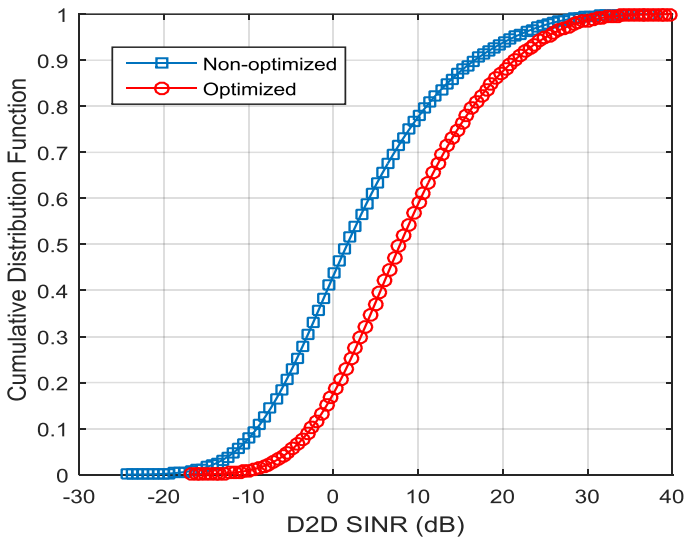

Figure 4.9 CDF of D2D system

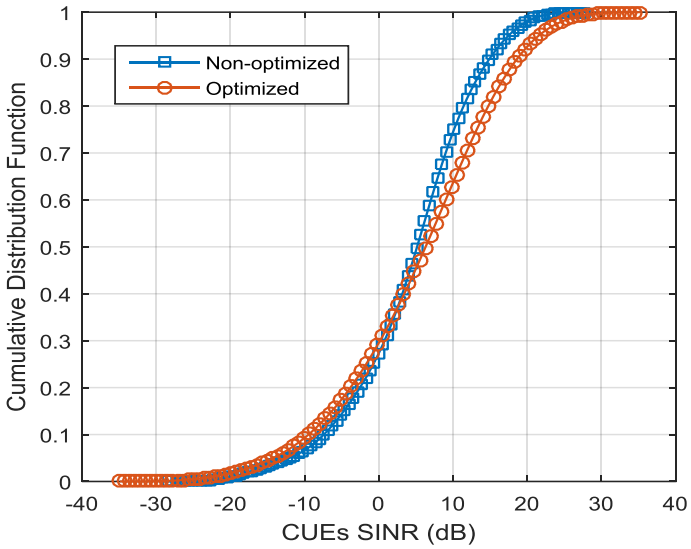

Figure 4.10 CDF of Cellular system

A comparison on the average SINRs for D2D and cellular systems before and after the optimization is shown in Figure 4.11, where the average SINR for the D2D system is show to be improved by 16.99% and the cellular system by 66.04%.

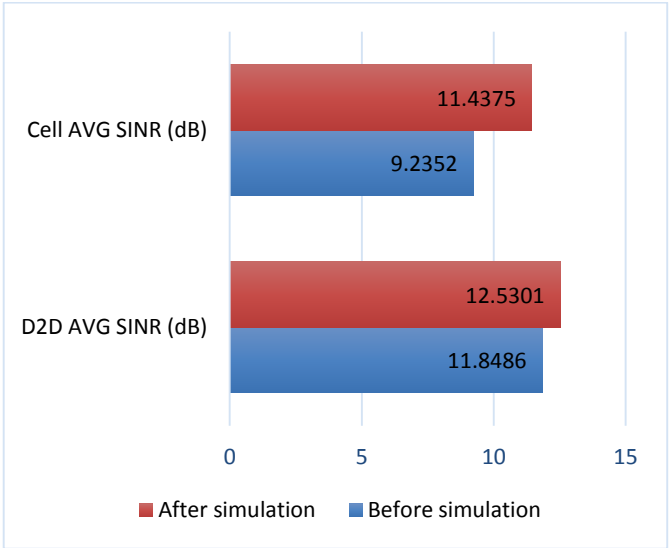

Figure 4.11 Average SINR comparison for D2D and cellular systems

To analyze these results, we observe the optimal power allocation vector obtained by the simulation, which is as follows:

$$\vec{P}_{optimal}(watts) = \langle 0.3, 0.2359, 0 \rangle$$

The high SINR region users will be allocated the max power, while the fair SINR region users are allocated 0.2359 watts, but more importantly, the low SINR region users are bound to switch off their transmission. This indicates that these users will not be able to meet the QoS requirements for good communication and thereby are switched to cellular mode. And that explains the higher improvement in the cellular system than that of the D2D system.

To evaluate the capacity of the network based on the obtained results, Figure 4.12 demonstrates a comparison for the results acquired in chapter IV with the results obtained in this section. To have a valid comparison, we considered only 2 D2D links and 1 CUE as the criteria for comparison. As a result, we observe a similar behavior of the transmitting capacities at the optimal power ratio P_d/P_b, i.e. $0.3/5 = 0.06$, which proves the accuracy of our algorithm.

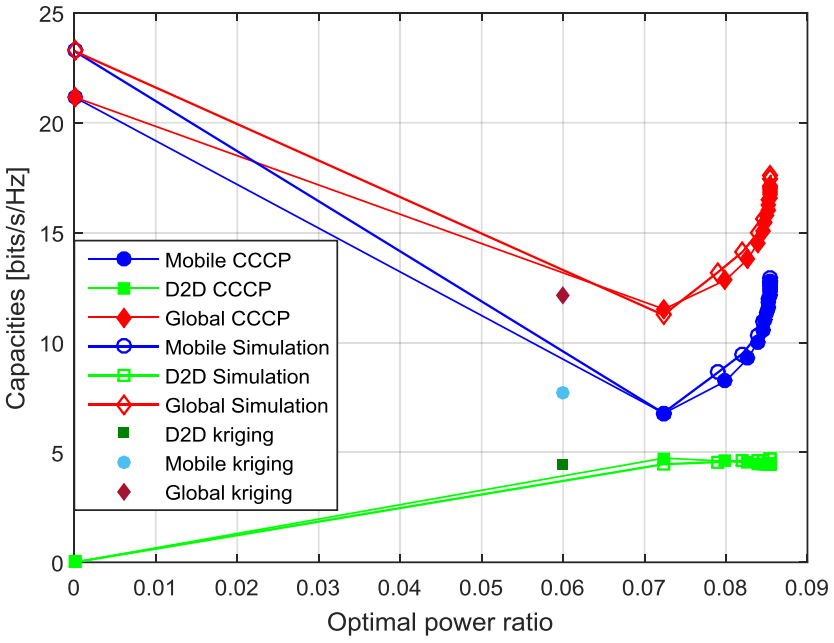

Figure 4.12 Comparison of the global, D2D and cellular capacities w.r.t the optimal power ratio for the proposed algorithms

So the problem of finding the optimal transmit power in D2D unerlaying cellular communications by using a spatial statistics proves to be not only accurate, but also feasible in most practical scenarios where extraction of sample data is difficult or impractical. Also, the model works smoothly in a dense network of multiple CUEs and D2D pairs occupying the same spectrum.

CHAPTER V

CONCLUSION

In this thesis, we studied the coexistence of D2D and LTE cellular networks by considering a non-cooperative deployment for the LTE and D2D links in a sense that full interference scenario is created. We derived closed-form expressions of the ergodic capacities for both systems based on their SIR distributions. Then, we showed that the capacities of both D2D and LTE are concave and convex respectively w.r.t the transmitted power ratio. We then proposed two optimization algorithms of the power allocation based on the CCCP and a Geo-statistical approach. The CCCP procedure is used to obtain the optimal transmitted power ratio that satisfies the target QoS under limited number of D2D links. In crowded D2D environment, the derived expressions become very complex and hence we proposed to exploit a spatial statistics technique to estimate the SINR and interference distributions based on the spatial correlation of the D2D links and cellular links using Kriging interpolator. The resulting information is then incorporated in the power optimization problem to obtain the optimal power allocations for the D2D transmissions, which maximizes the global capacity while guaranteeing the predefined QoS constraint. The analytical and numerical results demonstrated the effectiveness of the introduced algorithms and showed that there exists an optimal power allocation that leads to fair underlay operation in fully interfered heterogeneous networks.

BIBLIOGRAPHY

[1] K. David, D. Dixit and N. Jefferies, "2020 Vision," in *IEEE Vehicular Technology Magazine*, vol. 5, no. 3, pp. 22-29, Sept. 2010.

[2] M. N. Tehrani, M. Uysal and H. Yanikomeroglu, "Device-to-device communication in 5G cellular networks: challenges, solutions, and future directions," in *IEEE Communications Magazine*, vol. 52, no. 5, pp. 86-92, May 2014.

[3] Ying-Dar Lin and Yu-Ching Hsu, "Multihop cellular: a new architecture for wireless communications," *INFOCOM 2000. Nineteenth Annual Joint Conference of the IEEE Computer and Communications Societies. Proceedings. IEEE*, Tel Aviv, 2000, pp. 1273-1282 vol.3, Mar. 2000.

[4] Mumtaz, S. (2014). *Smart Device to Smart Device Communication*. J. Rodriguez (Ed.). Springer International Publishing.

[5] K. Doppler, M. Rinne, C. Wijting, C. B. Ribeiro and K. Hugl, "Device-to-device communication as an underlay to LTE-advanced networks," in *IEEE Communications Magazine*, vol. 47, no. 12, pp. 42-49, Dec. 2009.

[6] A. Asadi, Q. Wang and V. Mancuso, "A Survey on Device-to-Device Communication in Cellular Networks," in *IEEE Communications Surveys & Tutorials*, vol. 16, no. 4, pp. 1801-1819, Apr. 2014.

[7] J. Seppälä, T. Koskela, T. Chen and S. Hakola, "Network controlled Device-to-Device (D2D) and cluster multicast concept for LTE and LTE-A networks," in *IEEE Wireless Communications and Networking Conference*, Cancun, pp. 986-991, Mar. 2011.

[8] B. Guo, S. Sun and Q. Gao, "Downlink interference management for D2D communication underlying cellular networks – in *(CIC/ICCC), IEEE/CIC International Conference on Communications Workshops in China*, pp. 193-196, Aug. 2013.

[9] S. Wen, X. Zhu, Z. Lin, X. Zhang and D. Yang, "Optimization of interference coordination schemes in Device-to-Device(D2D) communication" in *7th International ICST Conference on Communications and Networking in China (CHINACOM)*, Kun Ming, pp. 542-547, Mar. 2012.

[10] D. Camps-Mur, A. Garcia-Saavedra and P. Serrano, "Device-to-device communications with Wi-Fi Direct: overview and experimentation," in *IEEE Wireless Communications*, vol. 20, no. 3, pp. 96-104, June 2013.

[11] S. Wen, X. Zhu, Y. Lin, Z. Lin, X. Zhang and D. Yang, "Achievable Transmission Capacity of Relay-Assisted Device-to-Device (D2D) Communication Underlay Cellular Networks," in *IEEE 78th Vehicular Technology Conference (VTC Fall)*, Las Vegas, pp. 1-5, Sep. 2013.

[12] J. Lianghai, A. Klein, N. Kuruvatti and H. D. Schotten, "System capacity optimization algorithm for D2D underlay operation," in *2014 IEEE International Conference on Communications Workshops (ICC)*, Sydney, NSW, pp. 85-90, June 2014.

[13] Y. Xu, Y. Liu, K. Yang, D. Li and Q. L. Bell Labs, "Interference mitigation scheme for Device-to-Device communication with QoS constraint," in *2013 IEEE 24th Annual International Symposium on Personal, Indoor, and Mobile Radio Communications (PIMRC)*, London, pp. 1784-1788, Sept. 2013.

[14] H. Min, J. Lee, S. Park and D. Hong, "Capacity Enhancement Using an Interference Limited Area for Device-to-Device Uplink Underlaying Cellular Networks," in *IEEE Transactions on Wireless Communications*, vol. 10, no. 12, pp. 3995-4000, Dec. 2011.

[15] H. Bawab, P. Mary, J. F. Hélard, Y. Nasser and O. Bazzi, "Ergodic capacity optimization in coexisting DVB-LTE-like systems," *2014 6th International Congress on Ultra Modern Telecommunications and Control Systems and Workshops (ICUMT)*, St. Petersburg, pp. 54-59, Oct. 2014.

[16] Jeffrey, A., & Zwillinger, D. (Eds.). (2007). Table of integrals, series, and products. Academic Press.

[17] Yuille, A. L., & Rangarajan, A. (2003). The concave-convex procedure.Neural computation, 15(4), 915-936.

[18] J. Riihijarvi and P. Mahonen, "Modeling Spatial Structure of Wireless Communication Networks," in *INFOCOM IEEE Conference on Computer Communications Workshops*, San Diego, CA, pp. 1-6, March 2010.

[19] D. M. Gutierrez-Estevez, I. F. Akyildiz and E. A. Fadel, "Spatial Coverage Cross-Tier Correlation Analysis for Heterogeneous Cellular Networks," in *IEEE Transactions on Vehicular Technology*, vol. 63, no. 8, pp. 3917-3926, Oct. 2014.

[20] Arpee, J., Gutowski, S., & Touati, M. (2004). U.S. Patent No. 6,711,404. Washington, DC: U.S. Patent and Trademark Office.

[21] C. Phillips, M. Ton, D. Sicker and D. Grunwald, "Practical radio environment mapping with geostatistics," in *2012 IEEE International Symposium on Dynamic Spectrum Access Networks (DYSPAN)*, Bellevue, WA, pp. 422-433, Oct. 2012.

[22] A. Konak, "Estimating path loss in wireless local area networks using ordinary kriging," *Simulation Conference (WSC), Proceedings of the 2010 Winter*, Baltimore, MD, pp. 2888-2896, Dec. 2010.

[23] Bohling, G. (2005) Kriging. [Online]. Available: http://people.ku.edu/ gbohling/cpe940/Kriging.pdf

[24] Kruisselbrink, J. W. (2010) Kriging. [Online]. Available: http://www.liacs. nl/_jkruisse/material/Kriging December 6 2010.pdf

[25] Johnston, K., Ver Hoef, J. M., Krivoruchko, K., & Lucas, N. (2001). Using ArcGIS geostatistical analyst (Vol. 380). Redlands: Esri.

[26] X. Luo, Y. Xu and Y. Shi, "Comparison of interpolation methods for spatial precipitation under diverse orographic effects," in *19th International Conference on Geoinformatics*, Shanghai, pp. 1-5, June 2011.